UNIVERSIDADE ESTADUAL PAULISTA "JÚLIO DE MESQUITA FILHO"
FACULDADE DE ENGENHARIA
CAMPUS DE ILHA SOLTEIRA

JESSÉ AUGUSTO DOS SANTOS PAIXÃO

DAMAGE QUANTIFICATION IN LAMINATED COMPOSITES USING GAUSSIAN PROCESS REGRESSION MODEL

ILHA SOLTEIRA
2020

JESSÉ AUGUSTO DOS SANTOS PAIXÃO

DAMAGE QUANTIFICATION IN LAMINATED COMPOSITES USING GAUSSIAN PROCESS REGRESSION MODEL

Dissertation presented to the Faculdade de Engenharia de Ilha Solteira - UNESP as a part of the requirements for obtaining the Master in Mechanical Engineering.
Knowledge area: Solid Mechanics.

Advisor: Prof. Dr. Samuel da Silva

ILHA SOLTEIRA
2020

FICHA CATALOGRÁFICA
Desenvolvido pelo Serviço Técnico de Biblioteca e Documentação

P149d

Paixão, Jessé Augusto dos Santos.
Damage quantification in laminated composites using gaussian process regression model / Jessé Augusto dos Santos Paixão. -- Ilha Solteira: [s.n.], 2020
86 f. : il.

Dissertação (mestrado) - Universidade Estadual Paulista. Faculdade de Engenharia de Ilha Solteira. Área de conhecimento: Mecânica dos Sólidos, 2020

Orientador: Samuel da Silva
Inclui bibliografia

1. Damage quantification. 2. Gaussian process. 3. Composite structures. 4. Structural health monitoring.

Raiane da Silva Santos
Raiane da Silva Santos
Supervisora Técnica de Seção
Seção Técnica de Referência, Atendimento ao usuário e Documentação
Diretoria Técnica de Biblioteca e Documentação
CRB/8 - 9999

UNIVERSIDADE ESTADUAL PAULISTA

Câmpus de Ilha Solteira

CERTIFICADO DE APROVAÇÃO

TÍTULO DA DISSERTAÇÃO: Damage Quantification in Laminated Composites using Gaussian Process Regression Model

AUTOR: JESSÉ AUGUSTO DOS SANTOS PAIXÃO
ORIENTADOR: SAMUEL DA SILVA

Aprovado como parte das exigências para obtenção do Título de Mestre em ENGENHARIA MECÂNICA, área: Mecânica dos Sólidos pela Comissão Examinadora:

Prof. Dr. SAMUEL DA SILVA
Departamento de Engenharia Mecânica / Faculdade de Engenharia de Ilha Solteira - UNESP

Carlos Alberto Cimini Jr.
Prof. Dr. CARLOS ALBERTO CIMINI JUNIOR
Departamento de Engenharia de Estruturas / Universidade Federal de Minas Gerais - UFMG

Prof. Dr. DAVID GARCIA CAVA
School of Engineering / The University of Edinburgh

Ilha Solteira, 31 de agosto de 2020

To my parents José and Marisa and to my sisters Josiane and Mirian
for their love and teachings throughout my life.

To my wife Giovanna
for her love, patience and unwavering support.

ACKNOWLEDGMENTS

First I would like to thank God for giving me the knowledge, ability, and opportunity to complete this research project. I'm extremely grateful for his blessings in my life.

I wish to express my deepest gratitude to my advisor Prof. Samuel da Silva for the unwavering guidance, patience, valuable advises, encouragement and friendship during the development of this research project. I would also like to extend my deepest gratitude to Prof. Eloi Figueiredo for the invaluable contribution to my work and for the support in the period I spent at Universidade Lusófona de Humanidades e Tecnologias. I'm also extremely grateful to Prof. Gyuhae Park for the helpful suggestions and support during my internship at Chonnam National University. I would also like to thank Prof. David Garcia Cava for providing the dataset of the wind turbine blade used in this work.

I would like to extend my sincere thanks to all my friends from the Group of Intelligent Materials and Systems (GMSINT). Many thanks to Carlos Santana ("Grilo") for assistance and friendship. Special thanks should go to my friends who shared the room with me: João Trentin, Luis Villani, Marcus Omori, Rafael Teloli, and Lucas Zanovelo. Thank you for always contributing to the good atmosphere in the office, the numerous pieces of advice during the development of my work, and the friendship. Thanks also to my friend Kayc Wayhs Lopes with whom I shared good talks about some of the challenges found in our projects and uncountable cups of coffee. Thanks also should go to Bruna Pavlack with whom I worked in the last months on the dataset of the wind turbine blade.

I would like to acknowledge the financial support provided by São Paulo Research Foundation (FAPESP) to this master project (grant number 2018/15671-1) and the research internship at Chonnam National University (grant number 2019/11755-9). I also acknowledge the Coordenação de Aperfeiçoamento de Pessoal de Nível Superior - Brasil (CAPES) - Finance Code 001, that financed part of this study.

My success and the completion of this work would not have been possible without the support and nurturing of my family to whom I dedicate this work. My parents Marisa and José for all the love and teachings throughout my life. My sisters Mirian and Josiane for the support in all my dreams. Finally, a huge thank you to Giovanna, my wife, for her love, patience and invaluable daily support!

RESUMO

Após detectar um dano em uma estrutura de material compósito laminado por meio de uma abordagem orientada a dados, o usuário precisa decidir se há uma falha estrutural iminente ou se o sistema pode ser mantido em operação sob monitoramento da progressão do dano e seu impacto na segurança estrutural. Neste cenário é essencial quantificar a extensão do dano para se tomar uma decisão. Portanto, este trabalho propõe uma metodologia para quantificação de dano baseada na aplicação de modelo de Regressão de Processos Gaussianos (GPR) para capturar a tedência e incertezas associadas a progressão do índice de dano global de acordo com a extensão do dano. O modelo GPR treinado de maneira supervisionada é utilizado para quantificar o dano através da interpolação estocástica dos índices de dano. Uma metodologia principal é proposta para quantificação de dalaminação em placas de compósito laminado utilizando índices de dano baseados no sinal de propagação de ondas Lamb. Modelos autoregressivos são aplicados para extrair características sensíveis ao dano e o algoritmo de distância quadrada de Mahalanobis é usado para calcular os índices de dano, embora diferentes técnicas de extração dos índices de danos possam ser adaptadas a metodologia. Para demonstrar a versatilidade da metodologia, uma versão modificada é apresentada com índices de dano baseados na análise espectral singular de sinais de vibração. Três aplicações experimentais são apresentadas para demonstrar a eficácia dessa abordagem – na primeira com uma placa de carbono-epóxi laminado com dano simulado e mudanças de temperatura para mostrar as etapas gerais do procedimento; na segunda envolvendo um conjunto de placas de polímeros reforçados com fibra de carbono com delaminação real causada em um ensaio de fadiga, para as quais a metodologia principal é aplicada; e, finalmente, um exemplo industrial envolvendo uma pá de turbina eólica com dano simulando a descolagem progressiva na borda de fuga, na qual aplica-se a versão modificada da metodologia proposta usando índices de danos baseados em sinais de vibração. O modelo GPR demonstra ser capaz de capturar a tendência e acomodar as incertezas relacionadas aos índices de dano versus o tamanho do dano nos pontos simulados nos testes. Os resultados demonstraram uma previsão adequada da área de delaminação simulada e real nas duas primeiras aplicações experimentais e da extensão de descolagem na pá de turbina eólica.

Palavras-chave: Quantificação de dano. Processos gaussianos. Estruturas de material compósito. Monitoramento de integridade estrutural.

ABSTRACT

After detecting initial damage in a composite structure through a data-driven approach, the user needs to decide if there is an imminent structural failure or if the system can be kept in operation under monitoring to track the damage progression and its impact on the structural safety condition. In this scenario, it is essential to quantify the extension and the damage's size to decide about these points. Therefore, this work proposes a damage quantification based on the application of the Gaussian Process Regression (GPR) model to capture the trend and uncertainties associated with the damage index progression according to damage extension. The GPR model trained in a supervised approach is used to quantify the damage by the stochastic interpolation of the damage indices. The central methodology is proposed for delamination area quantification in laminated composite plates using damage indices based on Lamb wave signals. Autoregressive models are applied to extract damage-sensitive features from Lamb waves signals, and the Mahalanobis squared distance is used to compute damage indices, although any damage features extraction technique could be used and adapted to the proposed methodology. A modified version of the central methodology is proposed to demonstrate the methodology's versatility, using damage indices based on singular spectrum analysis of vibration signals, a well-established technique in the literature. Three sets of tests are used to demonstrate the effectiveness of this approach — one in carbon-epoxy laminate with simulated damage under temperature changes to show the general steps of the procedure; a second test involving a set of carbon fiber reinforced polymer coupons with actual delamination caused by repeated fatigue loads, for which the central methodology is applied; and finally an industrial example involving a wind turbine blade with damage caused by debonding in the trailing edge and using traditional vibration-based damage indices. Various damage progression levels are measured during the tests and monitored using the sensors bonded to these structural surfaces. The GPR proved to be capable of capturing the trend and accommodating the uncertainties related to the damage indices versus the damage size in the simulated spots in the tests. The results manifest a smooth and adequate prediction of the size area of the simulated and real delamination damage in the two first application cases and the debonding size in the last application case.

Keywords: Damage quantification. Gaussian process. Composite structures. Structural health monitoring.

LIST OF FIGURES

LIST OF TABLES

LIST OF ACRONYMS

PZT	-	Piezoeletric transducer
SPR	-	Statistical Pattern Recognition
CFRP	-	Carbon Fiber Reinforced Polymer
DI	-	Damage Index
MSD	-	Mahalanobis Squared Distance
GPR	-	Gaussian Process Regression
NDE	-	Nondestructive Evaluation
SHM	-	Structural Health Monitoring
AR	-	Autoregressive
ARX	-	AutoRegressive with eXogenous input
AIC	-	Akaike information criterion
BIC	-	Bayesian information criterion
ASTM	-	American Society for Testing and Materials
RMSE	-	Root Mean Squared Error

LIST OF SYMBOLS

a_i	-	i-th coefficient of the autoregressive model
$\mathcal{A}$	-	polynomial containing the lag operator and cofficients of the autoregressive model
$\mathcal{A}_b$	-	polynomial containing the lag operator and coefficients of the autoregressive model identified in the baseline condition
$\mathbf{A}$	-	matrix of principal components
$\mathbf{C}_X$	-	covariance matrix of the embedded matrix
D_i	-	local damage index corresponding to the i-th path
$\mathcal{D}$	-	dataset composed of damage index and damage severity vectors
$\mathcal{DI}$	-	global damage index
$\mathbf{E}_X$	-	matrix of eigenvectors
$f(\cdot)$	-	Nonlinear regression function
$\boldsymbol{f}$	-	regression function relating damage index and damage severity
f_*	-	predicted output for a new input
$\boldsymbol{\mathcal{I}}$	-	identity matrix
$\mathcal{K}$	-	covariance matrix associated with the GPR model
$k(\cdot, \cdot)$	-	kernel function associated with the GPR model
$\bar{L}$	-	number of time sampling points of acceleration signal collected
L	-	length of acceleration signal into frequency domain
M	-	number of realizations of the signal vector
$\mathcal{M}$	-	Mahanobis squared distance
$p(\cdot\|\cdot)$	-	conditional probability function
$\mathbf{R}$	-	matrix of reconstructed components
$\boldsymbol{\mathcal{S}}$	-	vector of damage severity
$\mathbf{T}_B$	-	baseline feature matrix
$\mathbf{T}^i$	-	feature vector

x_i - i-th element of the vector of damage indices

x_j - j-th element of the vector of damage indices

$\mathcal{X}_1$ - damage sensitive feature based on the residual error

$\mathcal{X}_2$ - damage sensitive feature based on the coefficients of the autoregressive model

$\mathfrak{X}$ - vector of damage indices

$\mathbf{X}_m$ - signal vector into frequency domain of m-th realization

$\mathbf{X}_m$ - matrix containing signal vectors corresponding to the healthy condition

$\check{\mathbf{X}}$ - full embedded matrix of the reference state

y - time series data

$\mathbf{Z}$ - Test matrix in the Mahalanobis squared distance

w - hyperparameter of kernel function

W - number of legged copies used in the embedding operation

GREEK LETTERS

Λ_X	-	diagonal matrix of eigenvalues
$\boldsymbol{\theta}$	-	hyperparameter vector of kernel function
μ_B	-	mean vector of the baseline feature matrix
μ	-	mean vector of the training data in the baseline condition associated with Mahalanobis squared distance
ε	-	residual error of autoregressive model
ε_b	-	residual error of autoregressive model identified in the baseline condition
$\varepsilon_{\mathcal{S}}$	-	zero mean gaussian noise of the regression model
$\sigma^2(\cdot)$	-	variance operator
Σ	-	covariance matrix of the training data in the baseline condition associated with Mahalanobis squared distance
$\sigma_{\mathcal{S}}^2$	-	variance of the Gaussian noise associated with the regression model
σ_f	-	variance of the kernel function
Σ_B	-	covariance of baseline feature matrix

CONTENTS

1 INTRODUCTION

1.1 Context and Motivation

The use of composite materials has significantly expanded in the past decades. It has been driven by aerospace, automotive, agriculture, civil, and renewable energy industries due to its better properties than metallic materials, such as high strength and stiffness combined with a low-density and excellent corrosion resistance (GHRIB *et al.*, 2017). However, composite materials present a complex internal structure, usually anisotropic, and multiple types of damage that make the damage identification and prediction of a failure challenge. This leads to overdesigned and less cost-efficient structures, in order to avoid catastrophic failures (SAXENA *et al.*, 2011a). Traditional nondestructive evaluation (NDE) techniques are currently utilized for damage identification. However, they are often labor-intensive and may require disassembly of the structure, which increases the maintenance costs and system downtime, and it is usually limited to inspections when the structural degradation is suspected (YUAN, 2016). In this context, structural health monitoring (SHM) techniques have been the focus of intensive research and development in recent years as an alternative way for automatic and continual monitoring of composite structures even in service, reducing maintenance costs, downtime, and improving their safety and reliability.

SHM is defined by Larrosa, Lonkar and Chang (2014) as the diagnostic process to extract meaningful health information from a structure, based on the sensing data from distributed, permanently installed sensors at certain structural regions. In the classification proposed by Rytter (1993), SHM techniques present four functional levels: Level 1 - damage detection; Level 2 - damage localization; Level 3 - damage quantification, and Level 4 - estimation of the remaining useful life. In the literature, the first three levels are also categorized as diagnosis, during the last level as prognosis. Typically, the diagnosis, which is the focus of this work, includes an intelligent algorithm of signal processing from measurements in the structure to identify structural health's current state. Several SHM techniques for application in composite materials have been reported in the literature based on many different technologies such as ultrasonic inspection, imaging methods, acoustic emission, fiber optics sensors, piezoelectric transducers (PZT), and laser vibrometry (YUAN, 2016). Special SHM techniques based on active-sensing guided waves have attracted substantial attention in the past two decades, especially for composite structures due to the high sensitivity to incipient damage. However, due to their high sensitivity to operating/environmental conditions, active-sensing SHM methods still face significant challenges, which will be addressed in this work.

Composite materials present multiple types of damage, such as matrix-cracking, delamination, debonding, etc., which have a different impact on the performance of the structure (SAXENA *et al.*, 2011a). Nevertheless, the major concern is delamination damage, because it degrades the strength significantly and is usually the ultimate cause of the structural failure (LARROSA; LONKAR; CHANG, 2014). Many authors demonstrated the application of active-sensing with Lamb waves in composite structures for delamination diagnosis. Typically, an array of PZT attached in the structure is used to propagate Lamb waves transmitted by the examined material. The damage is identified by analyzing the received waves from multiple PZT sensors. Numerous methods have proved feasibility, especially for the levels of damage detection and localization (YUAN, 2016; TIAN; YU; LECKEY, 2015; FARRAR *et al.*, 2007; MITRA; GOPALAKRISHNAN, 2016). However, the damage quantification level is still little explored, which will focus on this work.

1.2 Literature Review

Lamb waves are a type of guided wave which propagates between two parallel surfaces of plate-like structures (IHN; CHANG, 2004). These waves are useful for SHM purposes due to its high sensitivity to small internal defects and capacity to inspect vast areas even in materials with high attenuation ratio such as composites (TIAN; YU; LECKEY, 2015). Some papers have been handled to explain the effects of interaction between damage and Lamb waves using numerical or data-driven identification models (TOYAMA; NODA; OKABE, 2003; RAMADAS *et al.*, 2009). Toyama, Noda and Okabe (2003) showed that transverse cracking and delamination decrease the stiffness of the structure and change the propagation velocity of the symmetric mode S_0 in cross-ply laminates. Ramadas *et al.* (2009) examined the interaction of the anti-symmetric mode A_0 with symmetric delamination, and the occurrence of mode conversion from A_0 to S_0 when the wave crosses the damaged region. They recommended that the time-of-flight between the through-transmitted mode-converted could be used to estimate the size of delamination. However, Lamb waves present numerous modes of propagation, and it is also influenced by a variety of interference sources, including high-frequency ambient noise, low-frequency structural vibration, temperature fluctuation, operational variability, inhomogeneity, and anisotropy of materials (SU; YE, 2009). Thus, the development of a robust SHM method depends on the extraction of a damage feature with reduced sensitivity to interference sources or a compensation method, which is a more sophisticated solution due to the Lamb wave propagation complexity.

In this context, numerous damage features are proposed in the literature involving the propagation velocity changes, amplitude attenuation, wave scattering, reflection, and others in the time or frequency domain (FIGUEIREDO *et al.*, 2012). However, the application of time-series predictive models, such as Autoregressive (AR) models, have been few explored for Lamb wave-based techniques, despite to be widely implemented in vibration-based SHM procedures since the last decade (SILVA; JUNIOR; JUNIOR, 2008; FIGUEIREDO *et al.*, 2012; NARDI *et al.*, 2016). Figueiredo *et al.* (2012) proved the capability of AutoRegressive models with eXogenous inputs (ARX) as a sensitive feature for damage detection in a composite plate. Silva (2018) illustrated some practical aspects of the implementation of ARX models using Lamb wave for system identification of a composite plate assuming temperature effects. Moreover, it was discussed the potential regarding the purpose of SHM.

Unfortunately, the scientific community has not extensively addressed damage quantification due to the limited understanding of the interaction mechanisms between guided waves and damage in composite structures (GHRIB *et al.*, 2018; TIAN; YU; LECKEY, 2015). Damage quantification is crucial to enhance the safety and the service life of composite structures, motivating the scientific community to develop some damage quantification methods. These strategies are not generic and are restricted to the typical damage found in composite structures: the delamination (LARROSA; LONKAR; CHANG, 2014). Tian, Yu and Leckey (2015) introduced a methodology for delamination quantification in laminated composites using wavenumber analysis. The results show that this procedure can be used not only for assessing the delamination area but also for the ply depth of the damage. Si and Wang (2016) proposed a damage identification technique based on a rapid multi-damage index algorithm. The damage quantification is achieved by applying a metric based on the energy density released extracted from the Hilbert spectral analysis of the Lamb wave signals, which presents a linear correlation with the delamination extent provided by polynomial regression. Paixao, Silva and Figueiredo (2020) used AutoRegressive (AR) models upon Lamb wave signals measured in a composite plate to compute damage-sensitive features for computation of indices using Mahalanobis squared distance. The quantification was achieved by training a set curve utilizing cubic spline functions to predict the delamination area. Silva *et al.* (2019) performed a related idea by manipulating the possibility of extrapolation of these trend curves to prognostic future states when the delamination grows in the same spot and with a similar effect. The results demonstrated that the features using AR models are accurately correlated with the structural state and a smooth trend that enables using cubic splines functions.

A practical obstacle to overcome is the natural variation of the measured signals caused by inherent uncertainties, e.g., imposed by operational and environmental conditions, sensor positioning, boundary conditions etc. (YADAV *et al.*, 2017). Some authors have exhaustively investigated those variations in the last few years. Yadav *et al.* (2017) used a multi-path unit-cell approach to propose a robust SHM approach for damage quantification using a curve of damage indices. A calibration procedure established by a hyperbolic tangent function was conducted in the training step, assuming severity changes within a similar aluminum plate set. Another set of plates was employed to observe the unknown damage severity and test the learned model. The simulated damage was a circular-cut introduced progressively by electrical discharge machining. Saxena *et al.* (2011a) suggested a similar procedure to damage quantification in composite structures. The tests were performed using the same dataset from the NASA prognostics data repository. More advanced probabilistic methods are recommended to treat data from composite materials. Corbetta *et al.* (2018) employed particle filters to realize the damage quantification and prognosis using the same dataset in the Carbon Fiber Reinforced Polymer (CFRP) coupons from NASA. Another not sufficient explored stochastic procedure to perform the same task in composite structures is the Gaussian Process Regression (GPR)(SAXENA *et al.*, 2011a). The GPR is a probabilistic nonlinear regression model and a helpful method for prediction with essential information about the uncertainty (FUENTES *et al.*, 2014). Recent works in the literature demonstrate its potential to mitigate the effects of operational variability on the damage detection level as reported by Valencia, Chatzi and Tcherniak (2020) and in the damage quantification and prognosis levels as reported by Chen, Yuan and Wang (2020) and Yuan, Wang and Chen (2019).

However, it should be noted that most of the damage quantification techniques are deterministic, which do not provide confidence intervals for damage size estimation and require a large amount of data from a population of identical structure to account for changing conditions (AMER; KOPSAFTOPOULOS, 2019). A stochastic approach to estimate the damage size would provide a more accurate and robust prediction with a reduced data footprint in this context. Recently, Corbetta *et al.* (2018) employed the stochastic method of particle filters, but focusing on the damage prognosis using the same dataset in the Carbon Fiber Reinforced Polymer (CFRP) coupons from NASA. As suggested by Saxena *et al.* (2011a), another not sufficiently explored stochastic procedure to perform the same task in composite structures is the Gaussian Process Regression, which will be employed in this work. The GPR is a probabilistic nonlinear regression, a helpful method for prediction with essential information about the uncertainty (FUENTES *et al.*, 2014). The GPR model's application is based on the assumption that there is a direct correlation between the defined damage index and damage severity, which is reasonable assumption verified for numerous damage indices and different application cases (YADAV *et al.*, 2020; GHRIB *et al.*, 2018; TIAN; YU; LECKEY, 2015; AMER; KOPSAFTOPOULOS, 2019). The GPR model can be applied to capture the defined damage index's trend and uncertainties related to the damage severity progression in a supervised learning approach under defined conditions. After training the GPR model, it can be used to monitor the damage severity progression inside the defined conditions using a stochastic interpolation using the damage index as an input of the model.

1.3 Problem Statement and Method of Approach

1.3.1 Main problem statement

In the main problem statement of this work, it is proposed the application of a new SHM methodology for damage quantification level in laminated composite plates under the simplified case of delamination propagation in a hotspot region, e.g., the potential location of delamination initiation is known a priori based on the historical data or other preliminary methods. Figure 1 provides the schematic idea of the problem statement.The main focus of the SHM system is to detect and estimate the delamination size. Despite the damage initiation of a hotspot region being a particular case, it is quite common in structures submitted to fatigue loading and a problem of great interest to the aerospace industry, as stated by Yadav *et al.* (2017).

The utilization of a GPR model for delamination area quantification in composite structures is proposed in this work, which is the central contribution of this research project. The best authors' knowledge is the first time to be applied in the damage quantification level for SHM procedures in composite structures. A secondary contribution is applying AR models for feature extraction from Lamb wave signals should also be noted, which, although not new, has been little explored in the literature despite the advantage of simplicity and successful, related applications in vibration-based methods of SHM. AR model identification of Lamb wave signals is used for feature extraction, and the damage indices (DI) are computed based on the Mahalanobis squared distance (MSD) set for a

Figure 1: Problem Statement.

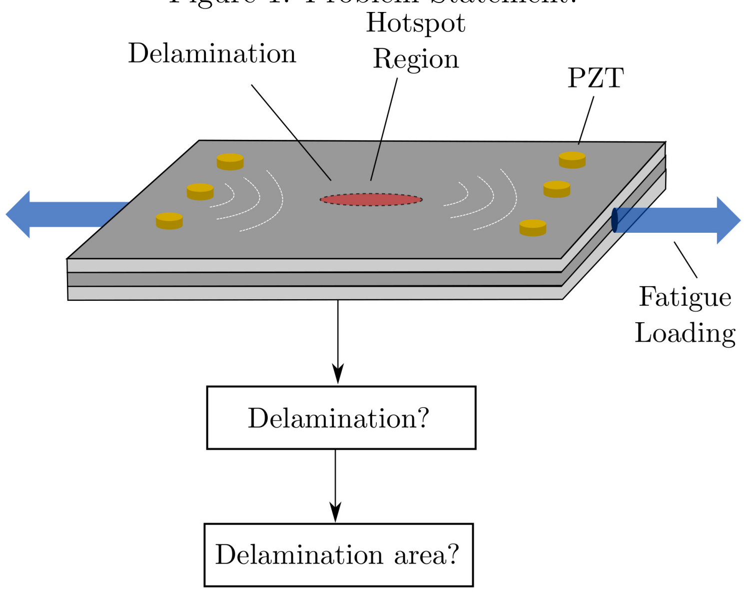

Source: Prepared by the author.

reference condition; then, the GPR model is trained to associate the damage indices with the delamination area.

Two applications are herein proposed to demonstrate the reliability of the methodology. First, a composite plate with progressive simulated damaged conditions is tested, in which the GPR model is trained and used in the same structure to predict intermediaries' delamination areas. Second, four similar CFRP composite coupons submitted to real progressive delamination states generated in a fatigue loading are tested. The GPR model is trained with three of them and tested to predict the last one's delamination area. The hypothesis here is that the learned model can be assumed for the quantification delamination area in identical structures for hotspot monitoring. This setup is the same used in Larrosa, Lonkar and Chang (2014) and Corbetta *et al.* (2018) in order to compare the performance.

1.3.2 Secondary problem statement

The GPR model's application is based on the assumption that there is a trend between the damage index and damage size, which is verified for different damage indices reported in the literature (YADAV *et al.*, 2020; GHRIB *et al.*, 2018; TIAN; YU; LECKEY, 2015; AMER; KOPSAFTOPOULOS, 2019). Then, it could be extended for different scenarios and techniques of damage feature extraction. In this context, the application of a modified version of the methodology used in the main problem statement addresses the damage quantification problem using vibration-based damage indices in an industrial example involving a wind turbine blade. Given a wind turbine blade instrumented with accelerometers to capture the impact response signals caused by an actuator, the SHM system's objective is to detect and estimate the debonding size in the adhesive joint of the blade.

The experimental application is proposed using the same dataset used by Garcia and Tcherniak (2019) that explored the damage detection level using vibration-based damage indices. Then, the damage indices proposed by Garcia and Tcherniak (2019) are combined with the application of the GPR model to address the damage quantification level. This practical application demonstrates the versatility of the proposed methodology based on the GPR model's application to be applied with different damage features extraction techniques and types of damage.

1.4 Objective

This research project aims to propose and validate an SHM methodology experimentally for damage quantification in composite structures based on the GPR model's application.

1.5 Main Contributions

The main contributions of the present work are the following:

- Development of a damage quantification methodology based on the GPR model application using Lamb-wave-based indices for hotspot monitoring of delamination in laminated composite plates(PAIXAO; SILVA; FIGUEIREDO, 2020).
- Application of damage features extraction method based on the AR model identification of Lamb-wave signals (PAIXÃO; SILVA, 2019);
- Proposition of a modified damage quantification methodology based on the GPR model application using vibration-based damage indices for SHM in wind turbine blades.

1.6 Outline

The work is organized as follows:

- **Chapter 1:** presents the motivation of this work, a literature review to contextualize the proposed methodology, the problem statement of this project, and the main objective of this research project.
- **Chapter 2:** describes the proposed methodology together with the theoretical background of the damage feature extraction process using the AR model and the application of the two machine learning algorithms proposed for damage detection and quantification.
- **Chapter 3:** presents a practical application of the proposed methodology in two application cases. In the first case, it is considered a unique CFRP plate with simulated delamination. In the second case, four CFRP coupons are tested with real delamination caused by fatigue loading. The results from the application of the methodology are discussed.
- **Chapter 4:** presents a modified methodology for damage quantification based on the application of the GPR model using vibration-based damage indices and an experimental application in a wind turbine blade.
- **Chapter 5:** the main conclusions are presented, and the next steps of this research project are outlined.
- **Appendix A - Details on the identification of Autoregressive models:** provides a complement of Chapter 2 by presenting the techniques applied for model order selection and validation.
- **Appendix B - Labview application:** shows the application developed in Labview to control the experimental setup in the application case I.
- **Appendix C - Publications:** presents the publications in the subject of this research project.

2 DAMAGE QUANTIFICATION METHDOLOGY BASED ON GPR MODEL USING LAMB WAVE-BASED DAMAGE INDICES

This chapter describes the methodology proposed for delamination area monitoring of the hotspot region in laminated composite plates. Firstly, Section 2.1 presents an overview of the SHM methodology proposed. Section 2.2 provides the theoretical background for applying the AR model to extract damage features from Lamb wave signals. In Section 2.3, the machine learning algorithms for statistical modeling and feature discrimination are presented and discussed. Then, in Section 2.4, a detailed description of the proposed methodology for the application in hotspot monitoring of the delamination area is carefully outlined. Finally, Section 2.5 presents the conclusions of this chapter.

2.1 Overview of the SHM methodology

The methodology proposed in this work can be cast in the context of the statistical pattern recognition paradigm (SPR) for SHM systems proposed by Farrar and Worden (2012), which is defined through a four-part process:

- Operational evaluation: involves the definition of the damage in the structure being investigated, the analysis and setting of limitations for operational and environmental conditions under which the system will be monitored.
- Data acquisition: comprises selecting the excitation method, the sensor types, number and locations, and the hardware for data acquisition.
- Feature extraction: to identify the data features that allow us to distinguish between healthy and damaged states of the structure.
- Statistical modeling for feature discrimination involves applying statistical techniques for discrimination between features from healthy and damaged conditions.

A more detailed discussion of the SPR paradigm can be found in Farrar and Worden (2012). The methodology proposed in this work focuses on parts 3 and 4 of the process, which have arguably received the most attention in the literature. An overview of the proposed methodology, according to the SPR paradigm, is presented in Fig. 2. The operational evaluation (part 1) has already been addressed on the problem statement in Chapter 1, where the type of damage is defined as delamination, and the conditions of monitoring are discussed. Also, most of the data acquisition (part 2) has been tackled once the methodology is based on the active-sensing of Lamb waves using PZTs, and the damage location is supposed to be known, which consequently defines the excitation method, type of sensors, and locations. The feature extraction process (part 3) is based on the application of the AR model for Lamb wave propagation signals identification. Damage sensitive features are extracted based on a comparison between statistical measures from coefficients and residual errors of AR models identified in a reference condition with those of a different condition, possibly damaged. In the statistical modeling (part 4), two machine learning algorithms are implemented: MSD for outlier identification in the delamination detection level; and the GPR model to estimate the delamination size.

Figure 2: Schematic representation of the methodology.

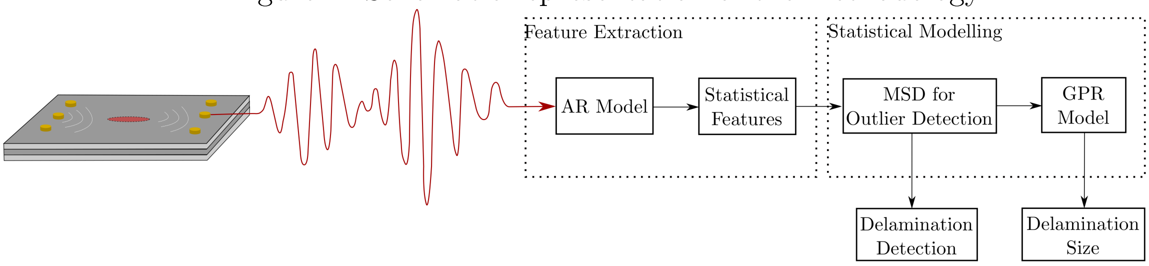

Source: Prepared by the author.

The application of this methodology for hotspot monitoring of the delamination area in laminated composite plates is based on the concept of statistical learning from training data. Initially, the machine learning algorithms for delamination detection and quantification have to be trained in a supervised learning approach using experimental data from known structural conditions by considering healthy and progressive damaged conditions. The MSD algorithm is trained to detect delamination by the identification of outliers values of the damage index. The GPR model is trained to capture the trend and uncertainties of the damage indices related to the delamination growth, which can be used to estimate the delamination area based on the damage indices using the stochastic interpolation provided the model. After that, the methodology can be applied to monitor the delamination area in laminated composite plates under the training conditions. The methodology's ultimate goal is to provide the capability to transfer the data-based knowledge of damage quantification from a single or a population of the representative laminated composite plate to other plates, or even scalable structural components.

2.2 Damage features extraction using AR models

The utilization of AR models in SHM has been extensively explored for vibration-based methods, especially for civil structures as bridges and buildings (FIGUEIREDO *et al.*, 2010). However, it has not been substantially utilized for Lamb wave-based propagation methods. The first application is reported by (LYNCH, 2005), which uses an ARX model to detect damage in an aluminum plate. Figueiredo *et al.* (2012) apply a similar for damage detection in composite plates and point out the advantages of using AR models, such as the reduced computational resources compared with frequency-based signal processing techniques. This makes the application of AR models very appealing for real-time health monitoring systems. In some recent papers, Silva (2018) addressed the use of time series methods for modeling narrowband signals of Lamb wave propagation and Cano and Silva (2020), demonstrated its effectiveness and suitability for damage detection.

The use of time series models to extract damage features from the signals in SHM applications is based on the capability of these models to capture the internal structure of time series, such as statistical correlations or systematic trends of varying time scales, which can be associated with the structural health state of the monitored system when compared with a reference state (PARK *et al.*, 2010). Therefore, regardless of the type of signal, if the presence of damage causes essential changes in the signal's internal structure, time series methods can be useful to detect it.

2.2.1 Model Identification

Given the time series $y(1), ..., y(N)$, a model that expresses $y(n)$ as linear combination of past p-th samples $y(n-1), ..., y(n-p)$ and residual error $\varepsilon(n)$ is called an AR model (KITAGAWA, 2010),

$$y(n) = \sum_{i=1}^{p} a_i y(n-i) + \varepsilon(n) \tag{1}$$

where p is the model order, $a_i, ..., a_p$ are the AR coefficients and $\varepsilon(n)$ is the residual error at the sample value n after fitting the AR model. The residual error is a portion of the signal that cannot be explained by the linear combination of the explanatory variables of the AR model, and it is assumed to be an independent random variable. If the AR model is adequately identified, the residual error follows a normal distribution with mean 0 and variance σ_ε^2 (KITAGAWA, 2010). For the representation of Equation 1 in more compact notation is convenient to define the operator lag q^{-k} the way that $y(n)q^{-k} = y(n-k)$, for which the following equation is obtained,

$$\mathcal{A}(q)y(n) = \varepsilon(n) \tag{2}$$

where $\mathcal{A}(q) = 1 + a_1q^{-1} + \cdots + a_pq^{-p}$ is the polynomial containing the lag operator and the coefficients of the model.

The AR model identification requires a priori the selection of the model order, which is initially unknown. Various techniques to address this problem have been proposed in the literature, and, among these, the Akaike information criterion (AIC) and Bayesian information criterion (BIC) have attracted much attention, especially in the literature focused on SHM. Although BIC is closely related to the AIC, the penalty term of BIC is a function of the data size, and so it is more severe than AIC, and it often presents a faster convergence (SILVA, 2017; FIGUREIDO, 2010). Therefore, BIC is used in this work to select the appropriate model order. More details about the model order selection procedure are presented in Appendix A.

Identification of AR models is a well-established research topic, and many identification methods have been developed in the literature, such as Yule-Walker, least-squares, and partial autocorrelation. The adequate performances of the least-squares method allied with its simplicity, low computational resources consumption, and robustness compared with other methods make it an appealing option for AR model identification (ZHENG, 2003). Therefore, the AR models are identified in this work using the least-squares method. A detailed review of these methods can be found in Kitagawa (2010).

2.2.2 Damage features extraction

The AR model application in SHM is based on the assumption that structural damage changes the structure's physical properties, which is reflected in the time-series response measured. In general, AR models are used as a damage-sensitive feature extractor based on two approaches: (1) using the residual errors; and (2) using the AR coefficients. In the first approach, the model is identified from the structure's signal in the baseline condition and used to predict the response obtained from a potentially damaged condition. As the damage will introduce changes in the structure response, the identified model will no longer accurately predict the response, which causes changes in the residual errors that can be used as a damage-sensitive feature. In the second approach, an AR model is identified for the baseline and damaged conditions. The AR coefficients are then used directly as a damage-sensitive feature to distinguish between the conditions (FIGUEIREDO *et al.*, 2010).

Suppose a measured signal from the Lamb wave propagation in a composite plate considering the baseline condition. The signal is identified by an AR model, which is described as follows :

$$\mathcal{A}_b(q)y_b(k) = \varepsilon_b(k) \tag{3}$$

where $\mathcal{A}_b(q) = 1 + a_{b_1q}^{-1} + \cdots + a_{b_p}q^{-p}$ is the new AR regressor polynomial and ε_b is the residual error in the baseline condition.

Note that if a signal from baseline condition is adequately identified and no significant changes are present in the signal, the parameters should be constant, and the residual errors should be white noise process. If a newly acquired signal under a different and unknown condition is identified using an AR model using the same selected order p, the identified model can be described by Eq. 2. Then, the new AR coefficients and residual errors change because the output signal is not the same in the new condition, and it carries new information. Various statistical features can be used to capture the changes in the distribution of coefficients and residual errors. In this work, using the two damage-sensitive features (i.e., coefficients and residuals) is recommended by using a statistical feature based on the variance, which has already been employed by Sohn and Farrar (2001). First, using the residual errors as follows:

$$\mathcal{X}_1 = \frac{\sigma^2(\varepsilon)}{\sigma^2(\varepsilon_b)} \tag{4}$$

where ε and ε_b are the vectors that contain all samples of residual errors from the AR models identified under an unknown and the baseline conditions, respectively. Second, using the AR coefficients in the form of:

$$\mathcal{X}_2 = \frac{\sigma^2(\mathcal{A})}{\sigma^2(\mathcal{A}_b)} \tag{5}$$

where $\mathcal{A}$ and $\mathcal{A}_b$ are the vectors containing the coefficients for the AR models identified under an unknown and the baseline conditions.

Once the features extraction process is defined based on the AR model identification, the structural health assessment can be addressed by the statistical modeling for feature discrimination. As the SHM algorithm's objective is the hotspot monitoring, the problem of the structural health assessment can be categorized into two levels: (1) damage detection; and (2) damage quantification. Note that for the hotspot monitoring problem, the damage localization is supposed to be known. Consequently, the damage localization is not necessary.

2.3 Damage detection

The damage detection level is addressed using the Mahalanobis Squared Distance (MSD), a distance measure for multivariate statistics outlier detection (WORDEN; MANSON; FIELLER, 2000). As two damage features are considered in the proposed approach, the MSD cast into a bi-variate space of features. The machine-learning algorithm based on the MSD is applied in the bi-variate feature space to compute the distance from the centroid of a well-known cluster of points to any other point. This cluster of points is defined by a training matrix $\mathbf{X} \in \mathbb{R}^{m\times 2}$ that is formed by the set of m samples of features $(\mathcal{X}_1 \quad \mathcal{X}_2)$ extracted from the conditions under the healthy state. As the algorithm is trained, one can compute the distance in the feature space to all l samples, defined by the test matrix $\mathbf{Z} \in \mathbb{R}^{l\times 2}$:

$$\mathcal{M} = (\mathbf{Z} - \mu)\,\Sigma^{-1}(\mathbf{Z} - \mu)^T \tag{6}$$

where μ is the mean vector and Σ, is the covariance matrix of the training matrix from the baseline condition $\mathbf{X}$.

Given that the instrumented structure with the PZTs presents l actuators and s sensors, this PZT network will provide $n = s \times l$ output signals from the n PZT actuator-sensor paths. The MSD is computed for each path independently, yielding a $\mathcal{M}$ vector n element.

$$\mathcal{DI} = \frac{1}{n}\sum_{i=1}^{n}\mathcal{M}_i \tag{7}$$

where MSD_i is the computed distance in the space of features assuming the i-th transducer path.

Once the $\mathcal{DI}$ is computed, the structural health classification can be implemented utilizing the outlier detection strategy by setting a threshold for the most significant $\mathcal{DI}$ value, considering all signals corresponding to the baseline condition.

2.4 Damage quantification using GPR model

In the quantification level of the methodology, it is proposed the application of a supervised machine learning algorithm employing GPR, also named by kriging. This non-parametric Bayesian approach has the benefit of working on small datasets and the ability to provide uncertainty measurements on the predictions. The goal here is to establish a direct ratio among the damage index and the surface delamination area in the structure using a GPR model. This model can learn the ratio and the uncertainties in the training step associated with environmental and/or operational variability, fabrication differences, defects, area measurements, etc., in order to predict the delamination area using a damage index extracted from a structure in an unknown condition. Another beneficial point to use GPR is calculating the variance that enables us to provide the confidence interval of the regression associating the damage index with the delamination area.

The surface area of delamination $\mathcal{S}^{(i)} \in \mathbb{R}$ can be written as an output of a nonlinear regression:

$$\mathcal{S}^{(i)} = f(\mathcal{DI}^{(i)}) + \varepsilon_{\mathcal{S}}^{(i)} \tag{8}$$

where $f(\cdot)$ is a nonlinear function, $\mathcal{DI}^{(i)} \in \mathbb{R}$ is an input vector, and $\varepsilon_{\mathcal{S}}^{(i)}$ is a zero mean Gaussian noise:

$$\varepsilon_{\mathcal{S}}^{(i)} \sim \mathcal{N}\left(\varepsilon_{\mathcal{S}}^{(i)} | 0, \sigma_{\mathcal{S}}^2\right) \tag{9}$$

where $\sigma_{\mathcal{S}}^2$ is a Gaussian noise variance with zero mean. For N tests, the training data set is:

$$\mathcal{D} = \left(\mathcal{DI}^{(i)}, \mathcal{S}^{(i)}\right)_{i=1}^{N} \equiv (\boldsymbol{\mathcal{X}}, \boldsymbol{\mathcal{S}}) \tag{10}$$

where $\boldsymbol{\mathcal{X}} \in \mathbb{R}^{N\times 1}$ is the input vector (damage indices) and $\boldsymbol{\mathcal{S}} \in \mathbb{R}^{N\times 1}$ is the output vector (delamination areas). Here the $\mathcal{S}^{(i)}$ is assumed to be the percentage of delamination area about the total area of the structure.

The function $f(\cdot)$ is assumed a priori as a Gaussian multivariate (RASMUSSEN, 2004):

$$\boldsymbol{f} = f(\boldsymbol{\mathcal{X}}) \sim \mathcal{N}(\boldsymbol{f}|0, \boldsymbol{\mathcal{K}}) \tag{11}$$

where $\boldsymbol{\mathcal{K}} \in \mathbb{R}^{N\times N}$ is the covariance matrix with $\mathcal{K}_{ij} = k(x_i, x_j)$, and $k(\cdot,\cdot)$ is the *kernel* function, also named by covariance function. The kernel function can assume different varieties depending on the treated problem. A general kernel function is the exponential kernel:

$$k(x_i, x_j) = \sigma_f^2 \exp\left[-\frac{1}{2}w^2\left(x_i - x_j\right)^2\right] \tag{12}$$

where $\boldsymbol{\theta} = [\sigma_f, w^2]$ is the hyperparameter vector that command the model's covariance. The hyperparameter is found by solving a maximization of a likelihood

$$p(\boldsymbol{\mathcal{S}}|\boldsymbol{f}) = \mathcal{N}\left(\boldsymbol{\mathcal{S}}|\boldsymbol{f}, \sigma_f^2\boldsymbol{\mathcal{I}}\right) \tag{13}$$

where $\boldsymbol{\mathcal{I}} \in \mathbb{R}^{N\times N}$ is the identity matrix. When a new input x_* is measured, using a bayesian inference, a new output f_* is identified by:

$$p(f_*|\boldsymbol{\mathcal{S}}, \boldsymbol{\mathcal{X}}, x_*) = \mathcal{N}\left(f_*|\mu_*, \sigma_*^2\right) \tag{14}$$

$$\mu_* = \boldsymbol{k}_{*N} \left(\boldsymbol{\mathcal{K}} + \sigma_S^2 \boldsymbol{\mathcal{I}}\right)^{-1} \boldsymbol{\mathcal{S}} \tag{15}$$

$$\sigma_*^2 = k_{**} - \boldsymbol{k}_{*N} \left(\boldsymbol{\mathcal{K}} + \sigma_S^2 \boldsymbol{\mathcal{I}}\right)^{-1} \boldsymbol{k}_{N*} \tag{16}$$

where

$$\boldsymbol{k}_{*N} = [k(x_*, x_1), \cdots, k(x_*, x_N)]$$

$$\boldsymbol{k}_{N*} = \boldsymbol{k}_{N*}^T$$

$$k_{**} = k(x_*, x_*)$$

The predictive distribution of $\mathcal{S}_*$ is similar to f_*, but σ_S^2 has the variance added. The hyperparameters are determined by using the likelihood of log-marginal using training data (MATTOS *et al.*, 2016):

$$\log p(\boldsymbol{\mathcal{S}}|\boldsymbol{\mathcal{X}}, \boldsymbol{\theta}) = -\frac{1}{2}\log\left|\boldsymbol{\mathcal{K}} + \sigma_S^2 \boldsymbol{\mathcal{I}}\right| - \frac{1}{2}\boldsymbol{\mathcal{S}}^T \left(\boldsymbol{\mathcal{K}} + \sigma_S^2 \boldsymbol{\mathcal{I}}\right)^{-1} \boldsymbol{\mathcal{S}} - \frac{N}{2}\log(2\pi) \tag{17}$$

A detailed discussion about the optimization methods of this function is given by Rasmussen (2004). A broad sensitivity is observed depending on the training data; a kernel function is chosen, regression order, and possible overparameterization. In this work, the UqLab software[1] was employed to optimize the kriging model (LATANIOTIS; MARELLI; SUDRET, 2015). The optimization of the hyperparameters is performed just to train the GPR model. After that, it can be used to estimate the delamination area just using as input the damage index.

2.5 Methodology description

The proposed damaged quantification methodology is illustrated in Figure 3 and can be split into two steps: 1) training and 2) test. In the training step, the supervised learning of the GPR model is performed using labeled training data from the structure under the

[1] `https://www.uqlab.com/`

baseline condition and known progressive damaged conditions. The set of training data consists of damage indices extracted from the output signals and the delamination area measured in the structure. The damage index is based on the MSD of two features ($\mathcal{X}_1$ and $\mathcal{X}_2$) extracted from AR models identified for the output signals. In the test step, a similar or the same structure in an unknown condition is interrogated about the presence of damage by performing an outlier detection test. When an outlier is detected, the delamination area is estimated from the damage index using the trained GPR model. In this work, each condition is defined by three pieces of information: a structural state that can be healthy or damaged; damage severity, which is the delamination area; and temperature changes in some cases. The condition referred to as the baseline is characterized by the structure in the healthy state, i.e., no delamination or ambient (or one specified) temperature.

Figure 3: Flowchart of the proposed methodology for damage quantification in composite structures.

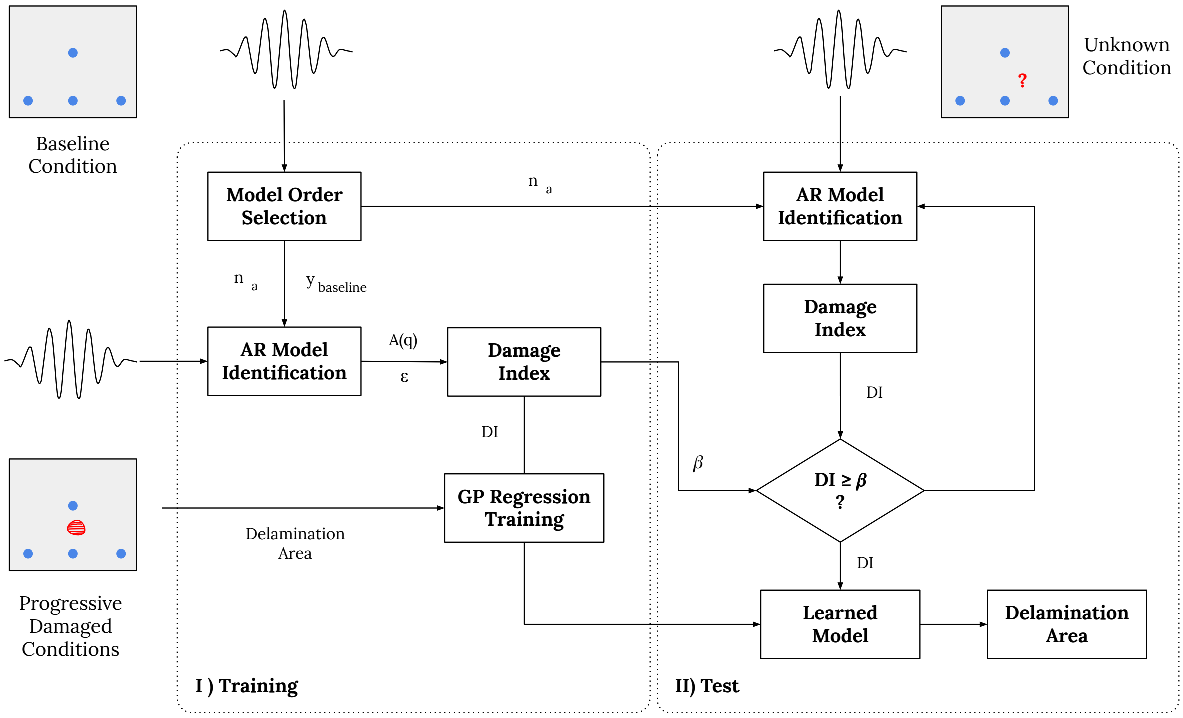

Source: Prepared by the author.

2.6 Conclusions

In this chapter, the methodology for hotspot monitoring of the delamination area in composite structures was presented. The procedure of damage-sensitive feature extraction based on AR models' application to identify Lamb wave signals were detailed. Then, two machine learning algorithms for damage detection and quantification were presented. The application of the outlier detection algorithm based on the MSD was proposed in the damage detection level. In the damage quantification, it was formulated the application of the algorithm for stochastic regression model GPR to map the delamination area as a function of the damage index extracted.

The methodology proposed can be used to monitor the delamination growth in hotspot regions of composite structures, where the potential damage location is known from historical data or other preliminary methods of analysis. This is a practical problem in the monitoring of structures submitted to fatigue loading. The methodology is based on the supervised learning of the machine learning algorithms, which requires a training step in controlled conditions of the delamination growth that can be expensive. However, it should be noted that the stochastic regression model's application can reduce the number of samples in the training dataset and provide a more robust prediction of the delamination area compared with ordinary deterministic methods of regression. The GPR model application for delamination size prediction allows us to adequately capture the uncertainties associated with the training step and improve the accuracy of the damage quantification in the structure's monitoring.

3 EXPERIMENTAL APPLICATION OF DAMAGE QUANTIFICATION METHODOLOGY BASED ON THE GPR MODEL IN CFRP COUPONS

This chapter presents the practical application and discussions of the proposed SHM method. Firstly, Section 3.1 describes the experimental setup of the two cases proposed. Section 3.2 shows the results obtained in the application of the proposed methodology for hotspot delamination monitoring. Finally, Section 3.3 presents the conclusions obtained in this chapter.

3.1 Experimental Setup

Two experimental application cases are used in this work to demonstrate the proposed approach. In the application case I, a carbon-epoxy composite plate with a unidirectional layup, is instrumented with four PZT transducers. Progressive damaged conditions are simulated by increasing the area covered by an industrial putty bonded on the surface's plate (SILVA *et al.*, 2019; PAIXAO; SILVA; FIGUEIREDO, 2020). In the application case II, four similar composite coupons with dogbone geometry are monitored during run-to-failure experiments under fatigue loading using two patches of six PZT transducers (LARROSA; LONKAR; CHANG, 2014). The experimental dataset used in this second case is available on the Prognostics Center of Excellence at NASA data repository[2](SAXENA *et al.*, 2011b).

3.1.1 Case I: CFRP plate with simulated damage

In this case, the CFRP plate is composed of 10 layers of carbon fibers unidirectionally aligned along a 0° direction and stacked in a matrix of epoxy resin. The dimensions of the plate are 500 x 500 x 2 mm^3. This material is commonly used in the aircraft industry, and it has been manufactured by a company in the sector, which has the name and the procedure of manufacturing omitted in this work due to intellectual property restrictions.

The composite plate is instrumented with four PZT transducers *SMART Layer* manufactured by *Acellent Technologies Inc*, each one measuring 6.35 mm in diameter and 0.25

[2] https://ti.arc.nasa.gov/tech/dash/groups/pcoe/prognostic-data-repository/

Figure 4: Composite plate and schematic view of the experimental setup (measurements in mm).

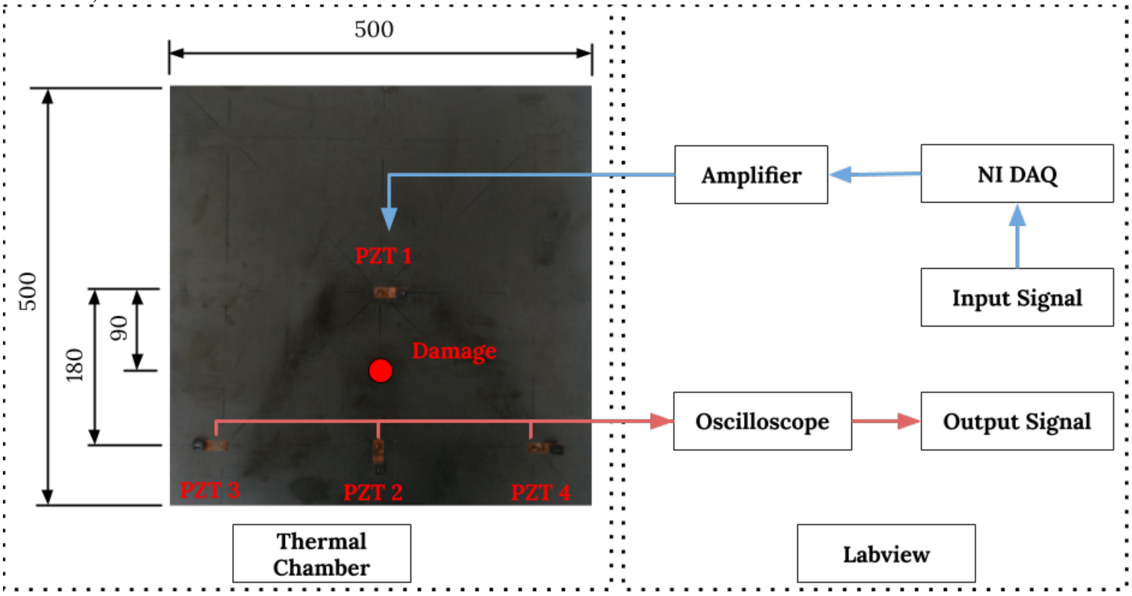

Source: Prepared by the author.

mm in thickness. The structure is excited by a five cycle sinusoidal tone burst with 35 V of amplitude and center frequency of 250 kHz applied on PZT 1. Then, PZT 2, PZT 3, and PZT 4 are used as sensors to acquire the output signal by using a sampling frequency of 5 MHz and timespan of 200 μs. The actuator signal is generated by NI USB 6353 from National Instrument coupled with a power amplifier EL 1225 from Mide QuickPack, and the output signal is acquired using an oscilloscope DSO7034B from Keysight. The application developed Labview and presented in Appendix B is used to control the generation/acquisition system. Figure 4 presents a schematic overview of the experimental setup used in the experiments.

Damage is simulated by inserting an industrial adhesive putty on the surface's plate. This additional localized mass simulates local changes in the plate's damping, which has some similarities to delamination in composites structures, as reported by Lee *et al.* (2011). A common practice in the literature is to simulate damage reversibly, i.e., without damnifying the structure. This will be discussed later and compared with the real delamination damage in application case II. The experiments were conducted inside a temperature chamber SM-8 Thermotron at seven temperature levels from 0°C to 60°C with a variation of 10°C in each level. The composite plate was placed in a free-free boundary condition in order to avoid operational variability.

The conditions tested are presented in Table 3.1.1. Healthy conditions are referred to as $H^{(t)}$ and damaged as $D^{(t)}_{(s)}$, where the superscript denotes the temperature of the test and

Table 1: Structural conditions tested for the carbon-epoxy laminate (case I).

	$H^{(t)}$	$D_1^{(t)}$	$D_2^{(t)}$	$D_3^{(t)}$	$D_4^{(t)}$	$D_5^{(t)}$	$D_6^{(t)}$	$D_7^{(t)}$	$D_8^{(t)}$	$D_9^{(t)}$	$D_{10}^{(t)}$	$D_{11}^{(t)}$
$\mathcal{S}$ [%]	0	0.196	0.282	0.384	0.502	0.785	1.13	1.53	0.95	2.01	2.27	2.54

Note: (t) superscript indicates the temperature of test in the range : 0, 10, 20, 30, 40, 50, 60 °C.
Source: Prepared by the author.

subscript s the number of damaged state. Baseline condition is defined as the structure in a healthy state at 30°C, represented by $H_{baseline}$. For each condition, 100 output signals were collected sequentially. The progressive damage conditions were simulated by the increase in the area covered with the putty, which has a circular format and constant mass.

3.1.2 Case II: CFRP coupons subject to tension-tension fatigue

Figure 5: CFRP composite coupon and schematic view of the experimental setup in the application case I (measurements in mm).

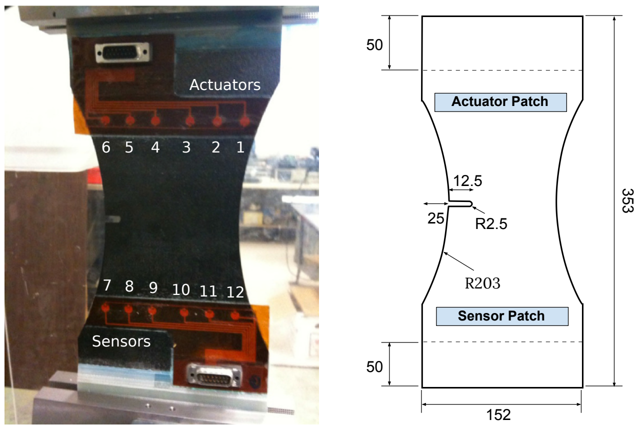

(a) (b)

Source: Adapted from Saxena *et al.* (2011b).

The dataset of the fatigue test experiments available on NASA data repository exhibits three types of CFRP laminates with different stacking sequences. Only one type of laminate is selected in this application case, which has the following stacking sequence: $[0_2/90_4]_s$. Four samples, labeled as L1S11, L1S12, L1S18, and L1S19, were manufactured with Torayca T700G unidirectional carbon-prepreg material. The structure presents a dogbone geometry with a side-notch element to induce stress concentration (see Figure 5).

The structure was instrumented with 12 PZTs *SMART Layer* from *Acellent Technologies Inc.* A pitch-catch configuration was used to monitor the wave propagation through the samples, where six transducers were used as actuators and the other six as sensors.

Figure 6: Output signals from path between PZT 4 and 9 considering baseline (H) and damage (D_8) conditions for the CFRP coupons (case II).

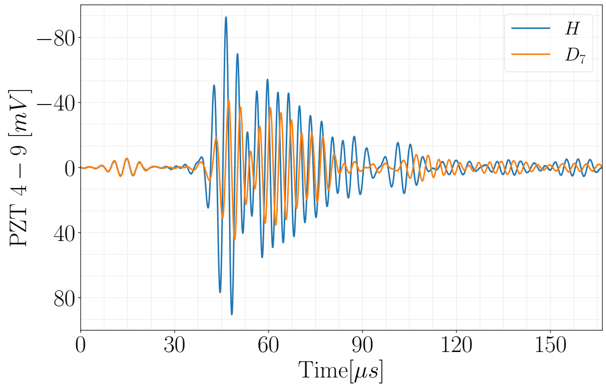

Source: Prepared by the author.

The input signal was a five cycles sinusoidal tone burst with an a°verage amplitude of 50 V. Seven frequencies were available on the dataset, from 150 kHz to 450 kHz, the frequency of 250 kHz was selected because as investigated by Larrosa, Lonkar and Chang (2014) the wave propagation presents the fundamental symmetric and anti-symmetric modes as distinguishable as possible according to dispersion curves. The signal acquisition and generation were performed using *Acellent's ScanScentry* hardware and *SmartPatch* interface software. Figure 6 illustrates an output signal in baseline condition versus one damage condition for the path between PZT 4 and 9.

The fatigue test was performed using an MTS machine and following the American Society for Testing and Materials (ASTM) Standards D3039 and D3479. The coupon samples were subjected to cyclic loading at a frequency of 5 Hz and a load ratio of approximately 0.14, with a maximum peak equal to 31 kN (LARROSA; LONKAR; CHANG, 2014; CORBETTA *et al.*, 2017). Periodically, the test was paused, and the coupon was removed from the machine, to perform the acquisition of signals from Lamb wave propagation in the structure and to collect X-ray images from the specimen in order to visualize the internal damage growth. The open-source image processing package *Fiji* was used to estimate the delamination area based on X-ray images, as already performed in previous works using this dataset (LARROSA; LONKAR; CHANG, 2014; CORBETTA *et al.*, 2017). Figure 7 illustrates the selected area to estimate delamination in the X-ray image. There is only one signal per path in this application case, i.e., there are only 36 signals per condition. To introduce significant variability, 50 signals per path were generated from the experimentally acquired ones by adding white noise with 40 dB relative to the output signal in the path with maximum power under the baseline condition. The conditions tested are presented in Table 2.

Figure 7: Example of X-ray image of composite coupon L1S11 under 40000 loading cycles and selected region of damaged conditions to estimate delamination area.

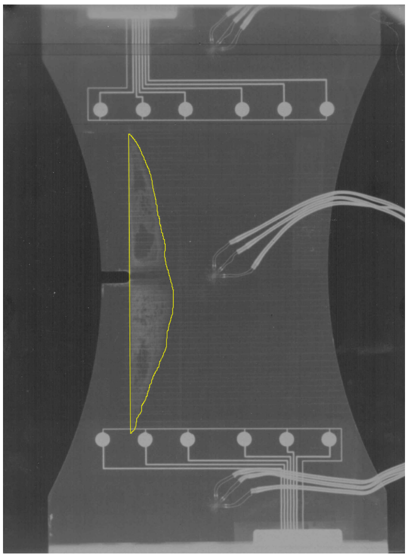

Source: Adapted from Saxena *et al.* (2011b).

Table 2: Structural conditions tested for CFRP coupons (case II).

Coupon	H	D_1	D_2	D_3	D_4	D_5	D_6	D_7	D_8	D_9
L1S11	0	0.23	0.33	0.44	0.84	1.84	2.35	2.84	3.25	4.22
L1S12	0	0.35	0.81	1.80	2.37	2.85	3.06	3.17	4.20	-
L1S18	0	1.32	1.87	1.82	2.49	2.95	3.08	3.09	3.57	-
L1S19	0	0.63	2.16	3.36	4.27	4.91	5.22	7.08	-	-

Source: Prepared by the author.

3.2 Application of the proposed methodology

The results and discussions from the application of the proposed SHM methodology in the two cases are presented together in this section in a complementary way by following the natural path in which the validation of the methodology was conducted in this research: first, case I under more controlled conditions with simulated damage and then, case II, with real damage. The proposed SHM methodology is divided into two steps: training and test. However, as most parts are executed in both steps, the results are presented simultaneously following the SPR paradigm parts presented in Chapter 2.

A detailed analysis of the effects of damage and temperature on the signal of wave propagation is presented first to provide a clearer understanding of the sensitivity of the damage in the feature extraction process. The effect of the simulated damage in the carbon-epoxy plate produced on the wave propagation is illustrated in Figure 8(a), where it can be identified a signal amplitude reduction as the area covered by the mass increases, which also increases the damping locally and causes a higher attenuation of the wave (LEE *et al.*, 2011). It is essential to note that this effect is more notable on the wave paths crossing the damage (between PZT 1 and PZT 2) and is dependent on the wave mode propagation. Furthermore, the effects of temperature changes on guided wave propagation have been under investigation by the scientific community, where a general conclusion is that temperature variations provoke a shift of phase and an amplitude variation in the signal compared with the baseline condition (SALAMONE *et al.*, 2009; SCALEA; SALAMONE, 2008). These effects are also demonstrated in Figure 8(b), where it can be observed that a temperature variation changes the amplitude and introduces a time delay in the response signal. Figure 9 presents the effect of real delamination damage in the CFRP coupons (case II). It is noted that variations in output signal under damaged conditions with progressive delamination area compared with baseline conditions. As damage severity progress, it is recognized a wave attenuation and a signal lag.

As observed in Figures 8(a) and 9, the effect of wave attenuation caused by the damage simulated with the industrial putty is similar to that caused by the actual delamination. Although the goal is not to establish a direct relationship between the simulated damage and a specific delamination area, the similar effects observed justifies the application of the proposed technique to simulate the damage in order to demonstrate the methodology under more controllable conditions.

Figure 8: Effects of damage (a) and temperature variation (b) on output signals from application case I: carbon-epoxy plate.

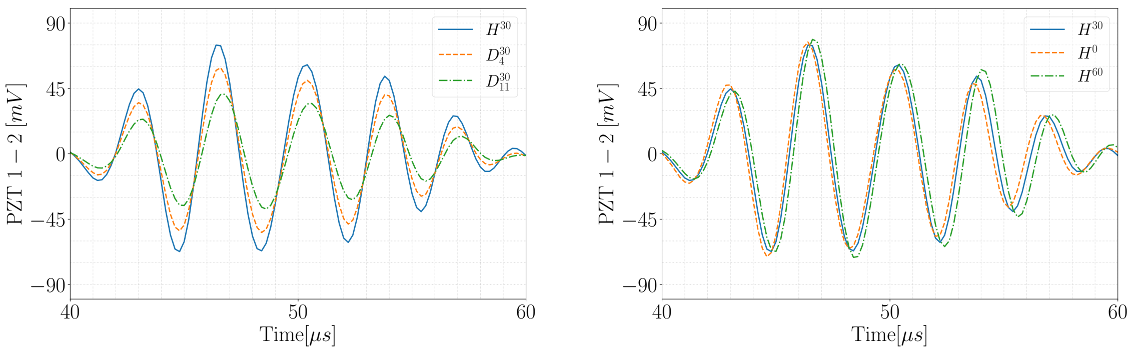

(a) Damage effect

(b) Temperature effect

Source: Prepared by the author.

3.2.1 Damage features extraction

First, the model order was selected based on BIC. The BIC for each path was evaluated according to the procedure proposed by Figueiredo *et al.* (2009). Appendix A detailed this issue. Since, the optimized model order did not present significant variations among all

Figure 9: Effects of damaged conditions on the output signal in the coupon L1S19 from application case II: CFRP coupon.

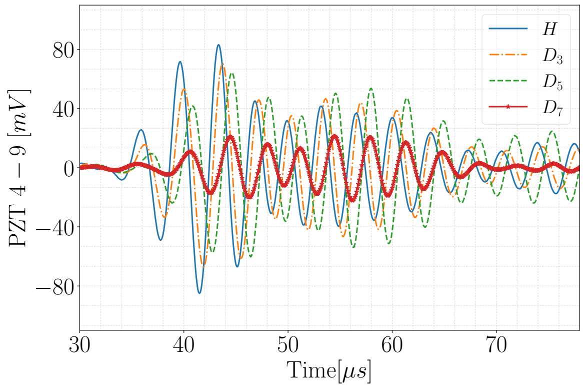

Source: Prepared by the author.

paths, as can be observed in the results presented in Appendix A, it was chosen a different model order for all transducer paths in each case. It was selected in the application cases I and II, a model order of 18 and 16, respectively.

Thus, each case has defined the model order used to identify an AR model for all acquired signals. The validation of each identified model was performed by comparing the model's prediction value with the measured signals and the autocorrelation analysis from residuals by considering the baseline condition. This procedure of AR model validation is detailed in Appendix A. Figure 10(a) shows the comparison of measured signal and predicted by the AR model for the application case I under the baseline condition. The residuals were tested based on the autocorrelation function; as observed in Figure 10(b), the prediction errors are from a white noise process, which suggests that the model has been adequately identified. The result of the model validation process was similar in both cases and for all evaluated paths. Therefore, for simplicity, due to a large number of paths, just the analysis of the path presented previously will be shown in this work.

After the AR model identification of the signals, the damage feature extraction using the residuals and coefficients were performed. Figure 11 shows the space of damage features extracted from the signals of the three paths in the application case I. A distribution pattern of the features related with the conditions can be noted, in the form of clusters, which is more pronounced for PZT 2, as a result of the damage localization. Compared with the cluster from the baseline condition, temperature variation shifts the cluster smoothly to the bottom right corner, increasing the variance of residuals related to the delay introduced in the signal and decreasing the variance of coefficients due to the smooth amplitude signal changes. On the other hand, damaged conditions shift the features to the left-side region of the baseline cluster; additionally, as the area of simulated

Figure 10: Baseline measured and predicted by AR(20) and autocorrelation of residuals for whiteness test validation within 95 % confidence bound (- - -) for the case I: Carbon-epoxy plate.

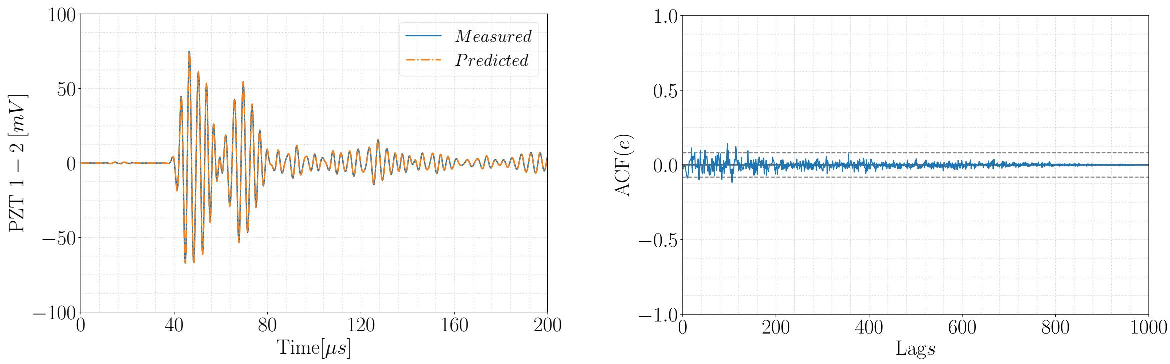

(a) Output signal

(b) Autocorrelation

Source: Prepared by the author.

damage increases, it moves to the lower region, which means a significant reduction on the residual and coefficients variance, as the simulated damage causes a significant attenuation of the amplitude signal in the path where the damage is placed. It is important to note that the model order was estimated for the baseline condition, and it was kept the same for each signal in all conditions; therefore, as the signal complexity increases when damage or temperature variation are introduced, the model can no longer fit the signal, and so the distribution of the residuals and coefficients change.

For application case II, Figure 12 shows the feature space for coupon L1S11 and two straight paths, one close and another far from the damaged region. In general, it can be observed a similar pattern from application case I, where the clusters of points under damaged conditions presented a reduction on the two features. It is important to note that this reduction is more pronounced for paths closer to the damage, and it is dependent on the delamination area, as demonstrated in Figure 14 by the damage indices computed. In this application case, the four coupons which present 36 paths each one presented the pattern demonstrated using the two selected paths shown in Fig. 12.

3.2.2 Damage detection

The damage feature pattern is now explored to classify the structure's condition using damage indices based on the MSD, trained using 70 % of data from the structure in the healthy state, including those with temperature variation. The ellipse of the confidence level of 95 % from the covariance matrix is presented in Figure 11 as well as the mean value of the cluster. Figure 13 shows, for the application case I, the damage index computed

Figure 11: Space of features for application case I.

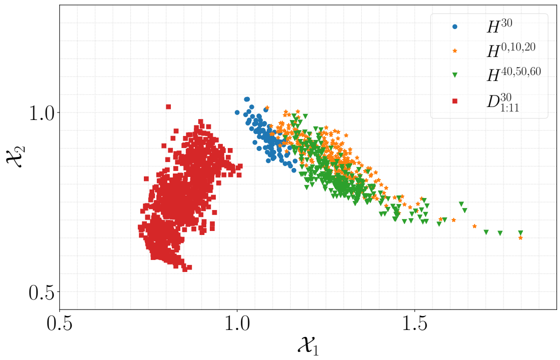

(a) PZT 2

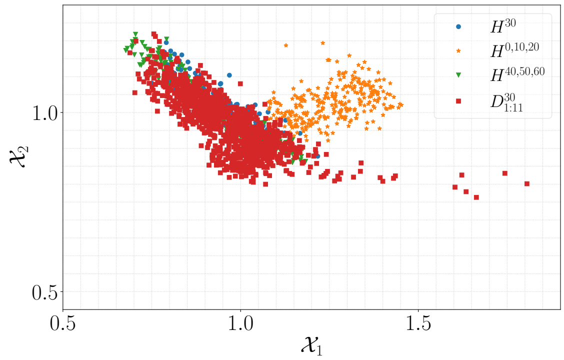

(b) PZT 3

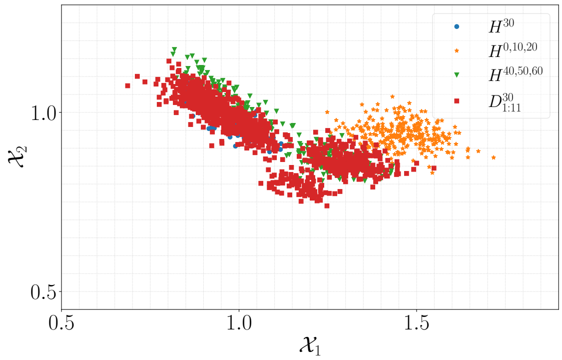

(c) PZT 4

Source: Prepared by the author.

Figure 12: Feature space considering the coupon L1S11 in two different paths (application case II).

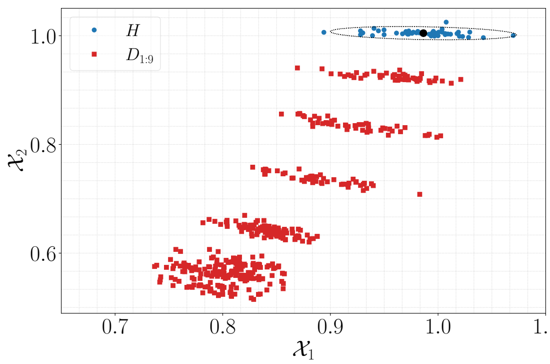

(a) PZT 5 - 8: Path through the damaged area

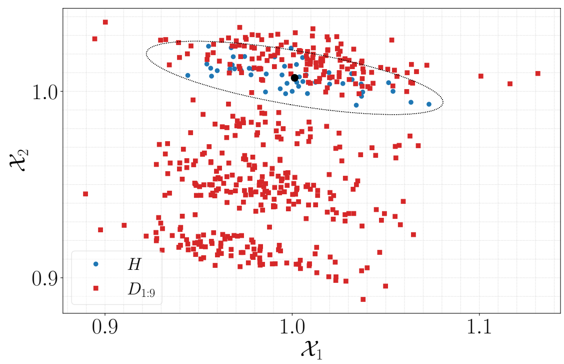

(b) PZT 2 - 11: Path ahead the damaged area

Source: Prepared by the author.

sequentially for all tested conditions, which is the average MSD from all three paths. As can be observed, the $\mathcal{DI}$ is capable of distinguishing damaged conditions from those of average and temperature variation and still capture the effect of simulated increasing delamination area. Figure 14 presents the damage index by delamination area for the coupon L1S11 in the application case II. It should be noted that in both cases, the damage index demonstrated to be well correlated with the delamination area, and it presents a smooth trend.

Figure 13: Damage index computed for all signals in application case I: carbon-epoxy plate.

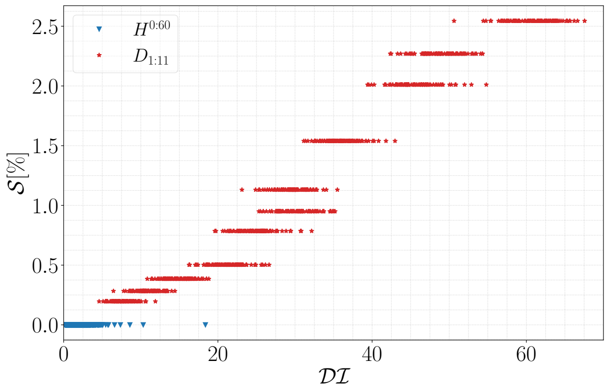

Source: Prepared by the author.

Figure 14: Damage index computed for all acquired signals from coupon L1S11 (application case II).

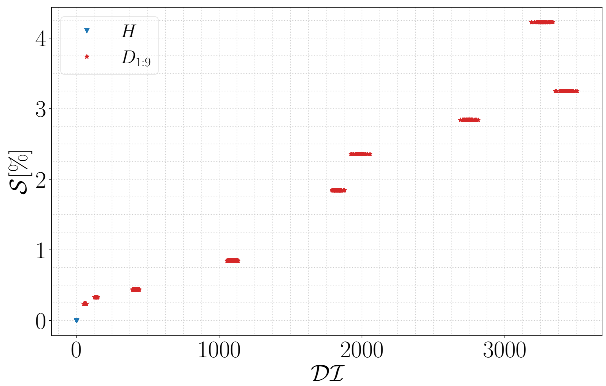

Source: Prepared by the author.

The damage detection was performed based on the proposed outlier detection strategy, where the threshold is defined as the most significant DI value under the healthy state. Table 3 summarize the results of the classification for the two cases. The percentages of true detections refer to the cases were the damaged states were correctly classified, and the false alarms indicate the cases where the damage was detected in the structure with no damage. In the application case I has observed a low rate of false alarms due to the conditions of temperature changes. However, the true detection rate still high. The classifier's performance in the application case II is maximum, with no false alarm and accurate detection. This is justified by the large variations in the damaged states' damage index compared with the healthy state. Furthermore, in this case, it was not considered changes in environmental or operational conditions.

Table 3: Results of the classifier performance for the two application cases.

	Case I	Case II
False Alarm [%]	1.8	0
True Detection [%]	99.9	100

Source: Prepared by the author.

The minimum delamination size detected was equivalent to a delamination area of 110 mm^2, which corresponds to 0.23 % of the surface area of the coupon L1S11. Due to Lamb waves' high sensitivity to small internal defects, it is expected to detect delamination area as small as that.

3.2.3 Damage quantification

Finally, Figure 15(a) illustrates the GPR of a progressive $\mathcal{DI}$ versus the area covered by the adhesive for application case I. The training of the GPR model associated $\mathcal{DI}$ with the percentage of the covered area $\mathcal{S}$ with a confidence interval of 3σ revealed a trend and an adequate estimative for intermediary test conditions. It should be noted that in this case, the training and test step were performed in the same structure. However, the data from different conditions were considered in the two steps, as indicated in Fig. 15(a).

On the other hand, for application case II, Figure 15(b) presents the stochastic interpolation considering as training data observations in coupon L1S19, L1S18, and L1S12 to obtain the kriging metamodel, i.e., the GPR model. The performance of the metamodel was tested with the observation measured in the coupon specimens L1S11. It is worth to note that all test data is inside the uncertainty bounds assuming 3σ, even assuming some possible imprecision to measure the delamination area in both cases during the training step. It is also important to note that in both cases was used a polynomial cubic trend with correlation function was chosen based on an exponential and ellipsoidal family, with optimization of the maximum likelihood estimation performed by gradient method to set the kriging metamodel (LATANIOTIS; MARELLI; SUDRET, 2015).

The validation of the GPR model prediction is presented in Figure 16 for both application cases. The estimated percentage of the delamination area using the damage indices from test conditions converged on the diagonal line. The Root Mean Squared Error (RMSE) computed for both cases, which were respectively 0.15 and 0.56, showed a better overall prediction performance in application case I compared with application II revealed by the lower RMSE value. The assessment of the prediction performance in each test condition is presented in Table 4, where it is showed the mean of the est values and the

Figure 15: Progressive $\mathcal{DI}$ versus simulated delamination area $\mathcal{S}$, and mean (—) of the kriging metamodel with confidence interval of 3σ (- - -).

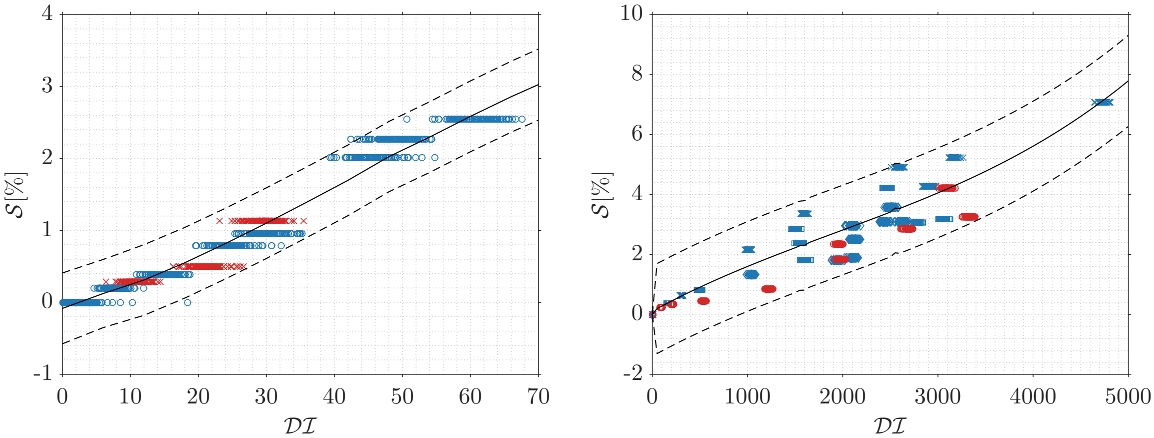

(a) Application case I - carbon-epoxy plate o training data and x test data

(b) Application case II - CFRP Coupons: training data are × L1S19, ⋄ L1S18 and □ L1S12, test data o L1S11.

Source: Prepared by the author.

Table 4: Mean of the estimated percentage of delamination and mean absolute error of prediction for test conditions in application cases I and II.

Condition	D3	D5	D8
Mean of estimated $\mathcal{S}$	0.27	0.70	1.04
Mean absolute error	0.06	0.20	0.12

(a) Application case I.

Condition	D1	D2	D3	D4	D5	D6	D7	D8	D9
Mean of estimated $\mathcal{S}$	0.21	0.34	0.78	1.72	2.61	2.79	3.72	4.66	4.43
Mean absolute error	0.02	0.02	0.34	0.87	0.77	0.43	0.88	1.41	0.20

(b) Application case II.

Source: Prepared by the author.

mean absolute error. As can be observed, the maximum values of the mean absolute error in application cases I and II were respectively 0.2 and 1.41. The higher mean absolute errors observed in application case II and consequently, the lower prediction performance of the GPR model is explained because, in this case, the model was trained and tested in different coupons, which involves more sources of uncertainties.

The GRP model's application to associate the $\mathcal{DI}$ with the damage size is based on establishing a functional relationship upon a supervised learning strategy. It has been explored for a particular case of hotspot monitoring of delamination. However, as long as a function describes the relationship between the $\mathcal{DI}$ and the damage size, the GPR model can be applied to learn and to predict the damage size in different scenarios. Then it could be extrapolated for applications in more complex structures and different types

Figure 16: Validation of the estimated percentage of delamination area with measured percentage of delamination area for test conditions in application cases I and II.The estimated percentage of delamination area (x) for all damage indices in each test condition and the mean of estimated percentage of delamination area (●) for each test condition.

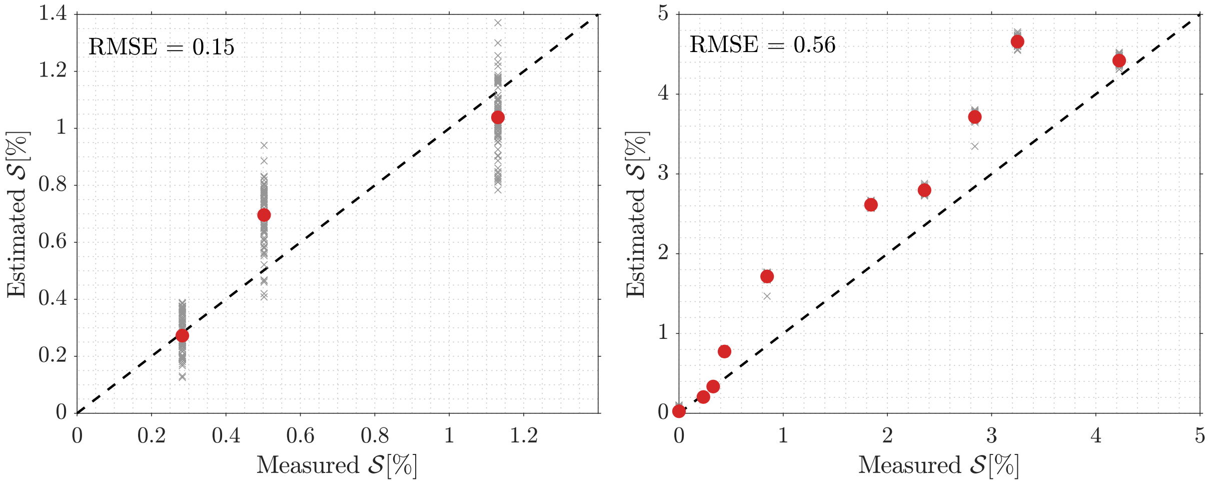

(a) Application case I - test conditions D3, D5 and D8.

(b) Application case II - all conditions from test coupon L1S11

Source: Prepared by the author.

of damage.

3.3 Conclusions

This chapter presented the application of the proposed SHM methodology for the problem of hotspot monitoring of delamination in composite structures. The damage feature extraction results based on AR models demonstrated an adequate sensitivity to the presence of the delamination and a direct correlation with the damaged area. Consequently, the simple classifier using the outlier detection strategy based on the damage index presented high performance. Many other damage features and detection methods are proposed in the literature. They could also be used in these levels; however, the application of time-series predictive models was chosen because few explored for wave propagation-based methods and their strong appeal for implementation on embedded microelectronics hardware, as already performed by Lynch (2005). The GPR model's application to establish the mapping relationship between the damage index and the delamination area demonstrated to capture the trend and uncertainties adequately. The trained GPR model performed well to estimate the delamination area in both cases: first, by considering the training and test on the same structure specimen and simulated damage, where the uncertainties caused by temperature variation were included in the healthy state; and second, for the training and test in different specimens nominally identical and real delamination induced by fatigue loading, which represents a more challenging case due to the higher uncertainty level and it is closer to the practical application of the method.

Although the application of the proposed SHM methodology presented herein was performed entirely in offline mode, in a practical implementation situation, the test step should be implemented online, allowing the hotspot monitoring in real-time. The results obtained with the GRP model's utilization reflect the central contribution of this work, applying a stochastic method to estimate the delamination area. It is essential to consider the Lamb wave signals' inherent uncertainties for damage quantification levels in composite structures. This can provide more accurate results than deterministic methods since the various sources of uncertainties discussed are inevitably in the practical application.

4 MODIFIED METHODOLOGY FOR DAMAGE QUANTIFICATION IN WIND TURBINE BLADES BASED ON THE GPR MODEL USING VIBRATION-BASED DAMAGE INDICES

The methodology for damage quantification proposed in Chapter 2 is based on the stochastic interpolation using the GPR model to capture the trend and uncertainties between the damage index and damage size. Although the application presented in Chapter 3 has been focused on a specific case of delamination quantification in laminated composite plates using Lamb wave propagation signals, it could be extended for different scenarios and damage feature extraction techniques. The methodology is adjustable to other damage feature extraction procedures, which could be more sensitive to damage in different applications.

The GPR model's application is based on the assumption that there is a trend between the damage index and damage size, which has been demonstrated in the application cases proposed in Chapter 3. This type of trend has been reported for different techniques of damage features extraction and other applications cases (YADAV *et al.*, 2020; GHRIB *et al.*, 2018; TIAN; YU; LECKEY, 2015; AMER; KOPSAFTOPOULOS, 2019). In recent work, Garcia and Tcherniak (2019) proposed a data-driven methodology for damage detection in large wind turbine blades using acceleration data. The methodology demonstrated to be useful for debonding detection in the trailing edge of blades. Also, the results demonstrated a monotonic increasing function of the damage index according to damage size progression. The damage index progression analysis suggests that it could be used for damage quantification, which is a problem of great interest to the clean energy industry because of the potential to improve the blades' operation and maintenance. In this context, in this chapter, the methodology proposed by Garcia and Tcherniak (2019) is extended for the damage quantification level based on the application of GPR model in a similar way to the methodology presented in Chapter 2. It demonstrates the versatility of damage quantification methodology presented in Chapter 2 for damage quantification based on the GPR model application using a different technique for damage feature extraction. Here, the damage features extraction method based on vibration signals proposed by Garcia and Tcherniak (2019) is used instead of the damage features extraction based on AR model identification of Lamb wave signals.

This chapter is organized as follows: firstly, a brief description of the methodology proposed by Garcia and Tcherniak (2019) and its extension for damage quantification based on the GPR model is given in Section 4.1. In Section 4.2, it is presented an overview of the experimental setup and procedures of data collection of the data set used for practical application in an SSP 34 m wind turbine blade. Then, the results and discussions obtained by the methodology's practical application are presented in Section 4.3. Finally, Section 4.4 presents the conclusions of this chapter.

4.1 Damage quantification using GPR model in wind turbine blades

The methodology presented in this section for damage quantification using the GPR model in wind turbine blades combines the methodology for damage detection proposed by Garcia and Tcherniak (2019) and the damage quantification methodology proposed in Chapter 2. As will be noticed, the methodology is a modified version of the methodology proposed in Chapter 2. This modified methodology proposed for damage quantification is illustrated in Figure 17 and can be split into two steps: 1) training and 2) test. Similar to the methodology presented in Chapter 2, the application of the GPR model still identical. In the training step, the GPR model's supervised learning is performed using labeled training data from the structure under the baseline condition and known progressive damaged conditions. In the test step, a similar or the same structure in an unknown condition is interrogated about the presence of damage by performing a hypothesis test with a defined threshold value. When damage is detected, the damage index is estimated from the damage index using the trained GPR model. The differences in this methodology compared with that proposed in Chapter 2 is restricted to the type of signal collected from the structure, which in this case is the acceleration of the impulse response instead of the Lamb wave propagation, and the methodology for damage detection, which is the same proposed and validated by Garcia and Tcherniak (2019).

4.1.1 Damage detection

The methodology proposed by Garcia and Tcherniak (2019) for damage detection in wind turbine blades is based on singular spectrum analysis. It is assumed a simple non-parametric method for data compression and information extraction (GARCIA; TCHERNIAK, 2019). The methodology is organized into four steps: data collection, creation of the reference state, feature extraction, and decision making. Figure 18 provides a scheme of the procedure, which will be summarized in the following subsections.

Figure 17: Flowchart of the proposed modified methodology for damage quantification based on GPR model using vibration-based damage indices.

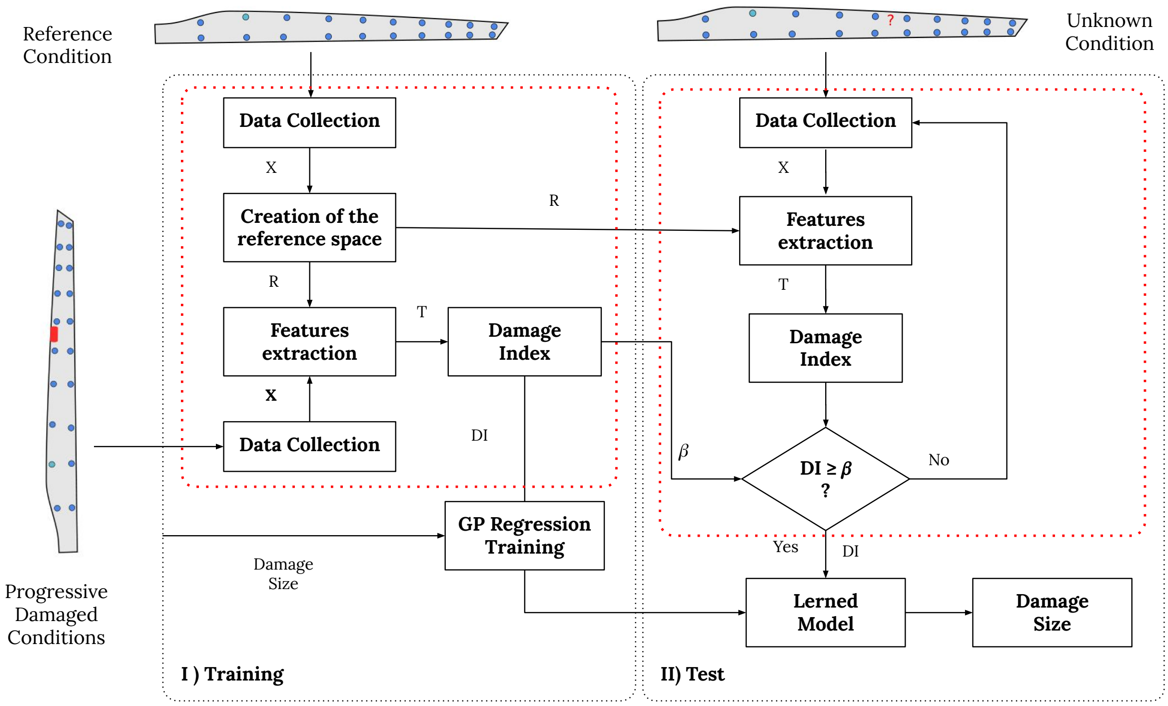

Source: Prepared by the author.

Data collection

In the data collection step, the discrete acceleration signals with $\bar{L}$ time sampling points collected from the structure are standardized to have zero mean and unit variance. Then, each signal is transformed to the frequency domain to obtain signal vectors $\mathbf{X}_m$ with length $L = \bar{L}/2$ where $m = 1, \ldots, M$ is the number of signal vector realizations measured as:

$$\mathbf{X}_m = (\mathbf{X}_{1,m}, \mathbf{X}_{2,m}, \ldots, \mathbf{X}_{L,m})^t \tag{18}$$

The signal vectors are stored in columns of the matrix $\mathbf{X}$ defined as:

$$\mathbf{X} = (\mathbf{X}_1, \mathbf{X}_2, \ldots, \mathbf{X}_M) \tag{19}$$

The matrix $\mathbf{X}$ presents dimension $[L \times M]$, and it is constructed for each healthy structural condition of the wind turbine blade. The matrix $\mathbf{X}$ corresponding to the healthy

Figure 18: Flowchart of vibration-based methodology for damage assesment in wind turbine blades proposed by Garcia and Tcherniak (2019)

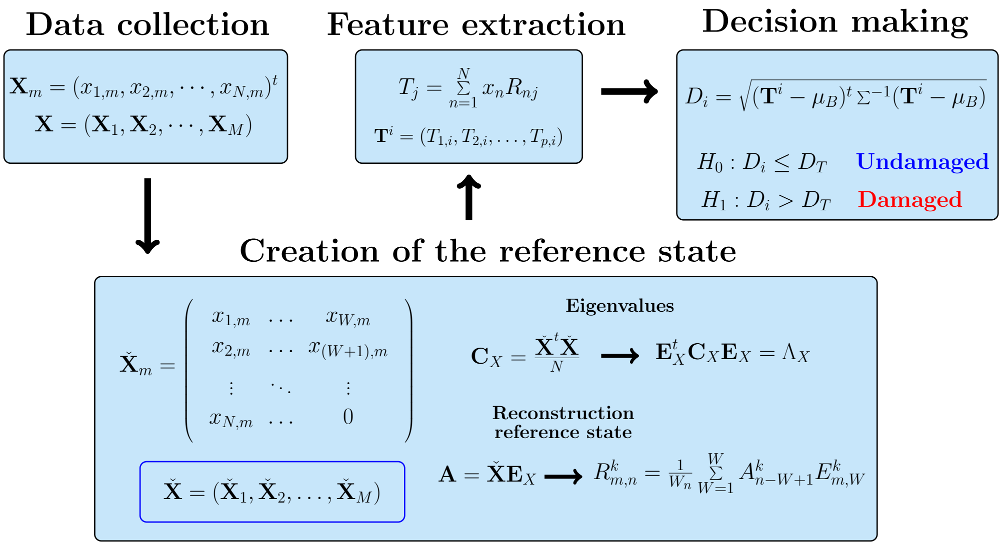

Source: Prepared by the author.

condition is used to create a reference state.

Creation of the reference state

The reference state's creation is performed using three operations: embedding the signal vector into a matrix with lagged copies, decomposition of the embedded matrix into principal components, and reconstruction of the reference state using a set of principal components.

In the embedding operation, a full embedded matrix $\check{\mathbf{X}}$ is created. Each element of this full matrix corresponds to a single embedded matrix $\check{\mathbf{X}}_m$ created by W-lagged copies of each vector signal $\mathbf{X}_m$. The dimension of each matrix $\check{\mathbf{X}}_m$ is $[L \times W]$, where W corresponds to the sliding window size.

$$\check{\mathbf{X}} = \left(\check{\mathbf{X}}_1, \check{\mathbf{X}}_2, \ldots, \check{\mathbf{X}}_M\right) \tag{20}$$

In order to compute the principal components of data it is necessary to perform the eigendecomposition of the covariance matrix $\mathbf{C}_X$ defined as follows, which has dimension

$[(MW) \times (MW)]$:

$$\mathbf{C}_X = \frac{\check{\mathbf{X}}^t \check{\mathbf{X}}}{N} \tag{21}$$

The eigendecomposition of $\mathbf{C}_X$ is written as:

$$\mathbf{E}_X^t \mathbf{C}_X \mathbf{E}_X = \Lambda_X \tag{22}$$

where Λ_X contains all eigenvalues stored in the diagonal matrix and $\mathbf{E}_X$ contains all eigenvectors $\mathbf{E}^k$ with dimension $\{\mathbf{E}^k : 1 < k \leq MW\}$.

The principal component $\mathbf{A}^k$ associated with each eigenvector $\mathbf{E}^k$ is computed by projecting the matrix $\check{\mathbf{X}}$ onto $\mathbf{E}_X$ as described by:

$$\mathbf{A} = \check{\mathbf{X}} \mathbf{E}_X \tag{23}$$

The reference state is formulated based on the reconstructed components obtained by the linear combination of a set of principal components. The reconstructed components are computed by convolving the principal components $\mathbf{A}^k$ with the associated $\mathbf{E}^k$:

$$R^k_{m,l} = \frac{1}{W_n} \sum_{w=1}^{W} A^k_{l-w+1} E^k_{m,w} \tag{24}$$

where W_n is a normalization factor described by

$$W_n = \begin{cases} n & 1 \leqslant n \leqslant W - 1 \\ W & W \leqslant n \leqslant N \end{cases} \tag{25}$$

The reconstructed components are arranged in columns into the matrix $\mathbf{R}$ with dimension $[L \times (MW)]$. Each column corresponds to the reconstructed component of the signal associated with the respective principal component. Therefore, $\mathbf{R}$ can be used as the reference state of the structure to which the observation signal vectors are compared (GARCIA; TCHERNIAK, 2019).

Feature extraction

In the feature extraction step, the similarity of each signal is compared with the reference state. It is performed by computing the feature vector defined in the following equation, which represents the inner product between each observed signal vector and the reference state's reconstructed components $\mathbf{R}$, where $j = 1, ..., W$:

$$T_j = \sum_{l=1}^{L} x_l R_{lj} \tag{26}$$

Inspection phase and decision making

A baseline feature matrix is constructed with a selected number of feature vectors from signals corresponding to the structure in the healthy state. This baseline matrix is defined in the following equation and it has dimension $[s \times u]$, where u is the dimension selected from the FV $\{\mathbf{T} : u \leq W\}$ and s is the number of signal vectors utilized to define the baseline matrix:

$$\mathbf{T}_B = \begin{pmatrix} T_{1,1} & T_{1,1} & \dots & T_{u,1} \\ T_{1,2} & T_{2,2} & \dots & T_{u,2} \\ \vdots & \vdots & \dots & \vdots \\ T_{1,s} & T_{2,s} & \dots & T_{u,s} \end{pmatrix} \tag{27}$$

Once the baseline feature matrix is defined, the damage index is computed based on Mahalanobis distance between all the observed feature vectors and the baseline feature matrix:

$$D_i = \sqrt{(\mathbf{T}^i - \mu_B)^t \Sigma_B^{-1} (\mathbf{T}^i - \mu_B)} \tag{28}$$

where μ_B is the mean row of the baseline feature matrix $\mathbf{T}_B$; Σ_B is its corresponding covariance matrix, and D_i is the damage index. It is important to note that the procedure described for damage index computing is based on the signals extracted from a single accelerometer. Therefore, it is considered a local damage index.

The structural health classification is performed based on the detection of outliers, which is necessary to define a local damage index threshold. As demonstrated by Garcia and Tcherniak (2019), the distribution of damage index in the reference state (observations from the healthy wind turbine blade) can be fitted by a log-normal probability density function. Then, the threshold is selected by a particular risk level (α), which determines the false alarm probability equal to the log-normal density function (GARCIA; TCHERNIAK, 2019).

4.1.2 Damage quantification

The damage detection methodology proposed by Garcia and Tcherniak (2019) is based on the local damage index D_i. Then, to extend its application for damage quantification level using the GPR model in structure instrumented with multiple sensors, it is convenient to define a new global damage index, which combines the features extracted from all paths. Otherwise, it should be necessary to train one GPR model for each sensor. Then, in an analogous way of the methodology proposed in Chapter 2, it is proposed here the following global damage index:

$$\mathcal{DI} = \frac{1}{N_s} \sum_{i=1}^{N_s} D_i \tag{29}$$

where N_s is the number of sensors used to monitor the structure.

The GPR model's application is proposed based on the methodology presented in Chapter 2 to extend the methodology proposed by Garcia and Tcherniak (2019) to the damage the quantification level. Again, the objective here is to use the GPR model to capture the trend and uncertainties of the damage index related to the damage severity. However, in this case, it is used as the new damage index, and the damage severity is assumed as the damage size of the debonded length in the wind turbine blade. Then, under the assumption that there is a nonlinear relationship between the damage index and damage size, the same formulation proposed in Section 2.4 can be applied here by considering the damage index defined in Eq. 29 and $\mathcal{S}$ as the damage size. As the formulation for the GPR model application still the same as that presented Section 2.4, it will not be presented here, and the reader is invited to consult that section for further details.

4.2 Experimental Setup

The dataset used in the experimental application proposed here belongs to Bruel & Kjaer, and Prof. David Garcia provided it. This dataset has been explored recently to validate different methodologies (GARCIA; TCHERNIAK, 2019; ULRIKSEN *et al.*, 2016; CRESPO, 2016). A brief description of the experimental setup will be given to provide a clearer understanding of the experimental application. A detailed description the experimental setup can be found in Nielsen *et al.* (2010).

The modified damage quantification methodology's experimental application is performed in the SSP 34 m wind turbine blade. The blade was manufactured by SSP Technology A / S, and the experiments were performed on a test rig at DTU Wind Energy facilities in Roskilde, Denmark. Figure 19(b) shows the wind turbine blade and the experiment facilities.

In the experiment, acceleration signals were collected for the blade's impact response under healthy and progressive damaged conditions. The electromechanical actuator produced the impact presented in Figure 19(c) positioned at four different positions. The four positions are indicated in Figure 19(a). Just at position A3, the actuator was placed inside the blade; it was placed on the surface outside the blade in other positions. The blade was instrumented with 20 triaxial accelerometers, model Bruel & Kjaer Type 4524-B, positioned as represented in the scheme in Figure 19(a). Ten accelerometers were placed on the trailing edge and ten on the leading edge. In total, 386 signals were collected for eight structural health conditions simulated (see Table 5).

The damage was artificially introduced to simulate the adhesive joint debonding, which is the leading cause of rotor blade structural collapse (MONTESANO; CHU; SINGH, 2016). This type of damage occurs when the adhesive bond between the laminates of the pressure and suction sides of the blade breaks, which can happen on both leading and trailing edges of the blade (GARCIA; TCHERNIAK, 2019). The damage was introduced in the region's leading-edge indicated in Figure 19(a). First, a series of holes through the adhesive between the blade's pressure and suction sides were drilled. Then, using a saw and a chisel, the holes were merged together, forming an opening that was gradually extended from 20 cm up to 120 cm by increments of 20 cm (GARCIA; TCHERNIAK, 2019). The debonded parts were connected by bolts, placed at 10 cm intervals. The healthy condition was then simulated by tightening all the bolts, and the progressive damaged conditions were reproduced by loosening some bolts. The number of loosened bolts was used to control the damage size.

Table 5: Damage size and number of signals measured on each experimental test condition.

Condition	Damage Size	Number of Signals
H	-	53
D20	20 cm	70
D40	40 cm	61
D60	60 cm	60
D80	80 cm	49
D100	100 cm	54
D120	120 cm	39
Total		386

Source: Adapted from Garcia and Tcherniak (2019).

Figure 19: Experimental setup of the SSP 34 m wind turbine blade.

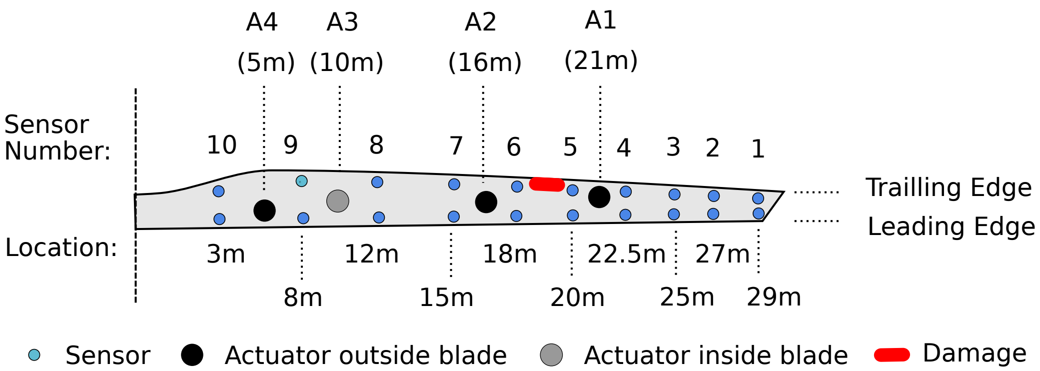

(a) Schematic of experimental setup

(b) SSP 34 m wind turbine blade

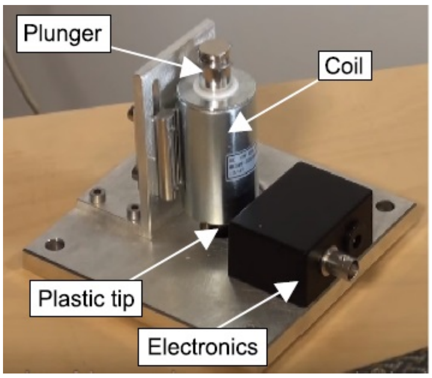

(c) Actuator

Source: Adapted from Garcia and Tcherniak (2019).

4.3 Results and Discussions

4.3.1 Damage detection

The methodology for damage detection described previously was applied in the dataset of SSP 34 m wind turbine blade. Although this dataset provides acceleration signals collected from sensors placed in the trailing and leading edges, it was considered just the data from the first region supported by the conclusion of the best damage detection performance for the accelerometers placed along the trailing edge as reported by Garcia and Tcherniak (2019). In that study, the authors defined the parameters chosen for the best methodology performance, which were employed in this work. In the creation of the reference state, it was considered $M = 10$ signal vector realizations with a sliding window size of $W = 10$. The feature vector dimension was set to $u = 5$. The baseline matrix construction was performed using $s = 26$ feature vectors of dimension $u = 5$ extracted from healthy condition signals. In the inspection phase, the risk of false alarm probability was set to $\alpha = 0.01$. A detailed discussion of each one of these parameters on the methodology performance can be found in Garcia and Tcherniak (2019).

Figure 20 presents a comparison between the measured and reconstructed spectrum frequency of the reference state considering the signal collected by the accelerometer one and actuator position at A1. As can be observed, it can be observed that the use of 5 principal components allows an adequate reconstruction of the spectrum frequency, which is used as the reference state.

Figure 21 shows the damage index by damage size obtained considering the accelerometers in the trailing edge for each actuator position. As can be observed, the damage sensitivity depends on the observed sensor and actuator location. The actuator at position A3 provides a lower sensitivity, and the damage index computed for damaged conditions is harshly distinguishable from the healthy condition. As shown in Figure 21(c), most of the damage index for damaged conditions is still below the threshold value, indicating poor classification performance. A higher damage sensitivity is noticed at actuator positions A1, A2, and A4, as can be noticed by increasing the damage index for damaged conditions compared with the healthy condition. A detailed discussion of the classifier performance is provided in Garcia and Tcherniak (2019), where it is demonstrated that when the excitation was performed on the actuator location A1 and A2, which are the closest to the damage and the tip of the blade, the percentage of true negatives and true positives is higher for the majority of the accelerometers along the trailing edge.

Figure 20: Reconstructed reference state and measured spectrum frequency under healthy condition obtained from signals measured by accelerometer 1 in trailling edge and actuator location at A1.

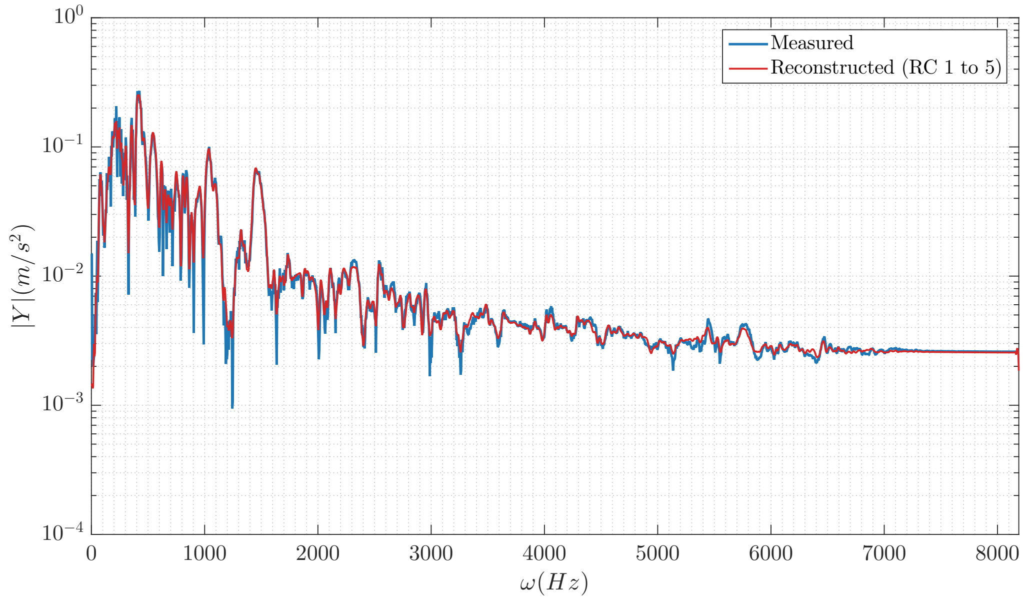

Source: Prepared by the author.

4.3.2 Damage quantification

The damage quantification methodology was performed using the global damage index proposed in Eq. 29. It merges the local damage indices' information from all paths into a unique damage index for each actuator position. The global damage index computed was used as input of the GPR model. The GPR model's training step was considered the global damage index of the following conditions: H, D40, D80, D100, and D120. The damaged conditions D20 and D60 were used in the test step to validate the damage size prediction using the GPR model. The GPR model training set a polynomial quadratic trend with correlation function chosen based on the ellipsoidal type and exponential family, with optimization of the maximum likelihood estimation performed by gradient method (LATANIOTIS; MARELLI; SUDRET, 2015).

Figure 22 exhibits the stochastic interpolation obtained using the trained GPR model represented by the mean and 95 % confidence interval of the predicted distribution. As can be observed, most of the damage indices used in the training and test steps are inside the confidence interval region, suggesting an adequate selection of training parameters. It is important to note that the global damage index presents a clear monotonic increasing trend captured by the GPR model.

The validation of the GPR model prediction for the test conditions D20 and D60 is

Figure 21: Damage index by damage size for accelerometers in the trailing edge for actuator positions (a) A1, (b) A2, (c) A3 and (d) A4. The damage index in the healthy(●) and damaged conditions(●) The dashed line (- - -) corresponds to the threshold defined by a risk of false alarm probability equal set to $\alpha = 0.01$

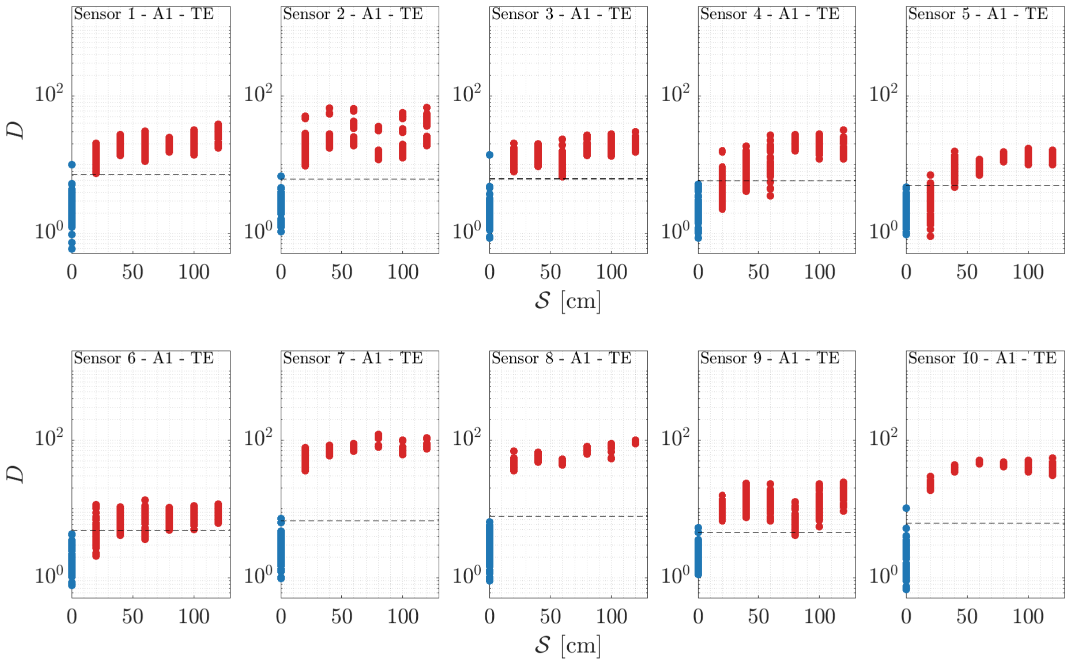

(a) Actuator Position A1

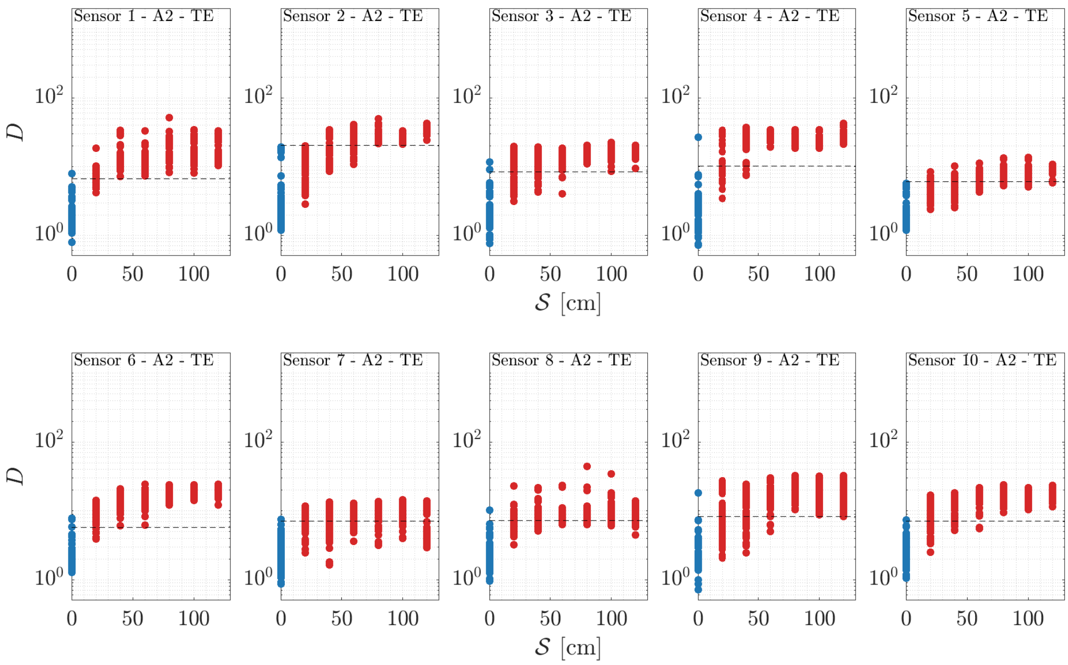

(b) Actuator Position A2

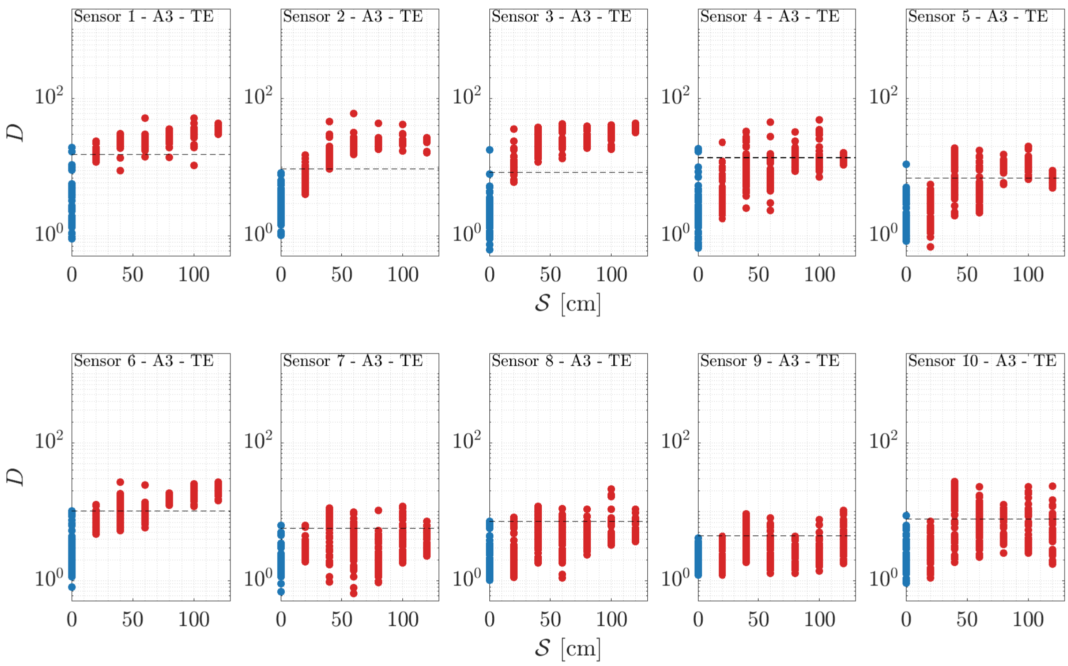

(c) Actuator Position A3

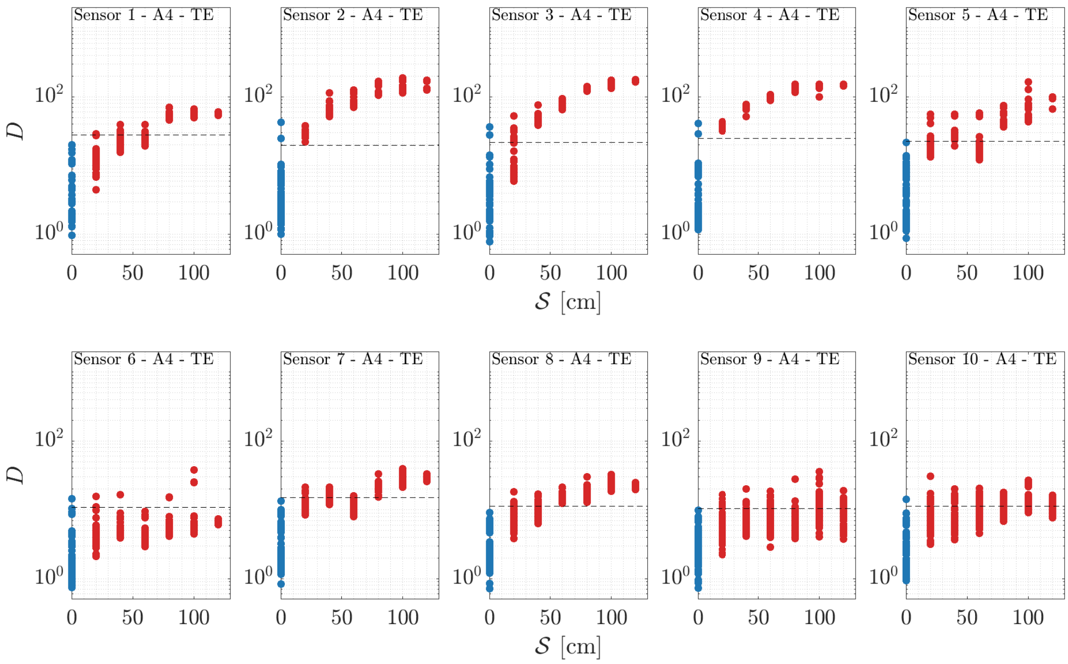

(d) Actuator Position A4

Source: Prepared by the author.

Figure 22: Stochastic interpolation of global damage index for each actuator position by damage size. The GPR model was trained using five conditions (●) and tested with two conditions(●). The bold line (—) corresponds to the mean and the gray colored region (■) to the 95 % of confidence interval predicted by the GPR model.

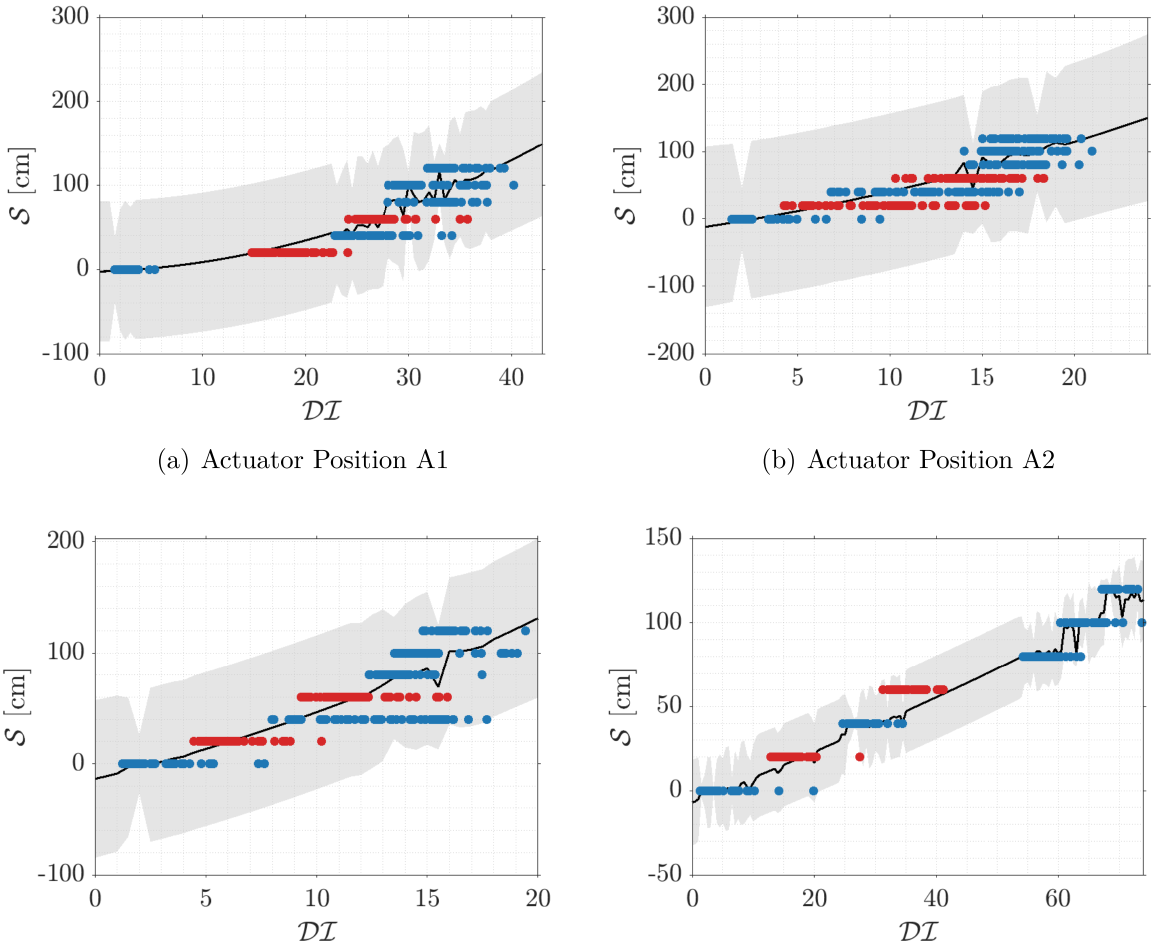

(a) Actuator Position A1

(b) Actuator Position A2

(c) Actuator Position A3

(d) Actuator Position A4

Source: Prepared by the author.

Figure 23: Validation of estimated damage size using the GPR model by the actual damage size for each actuator position and test condition. The estimated damage size for all damage indices (x) and the mean of estimated damage size (●) for each test condition.

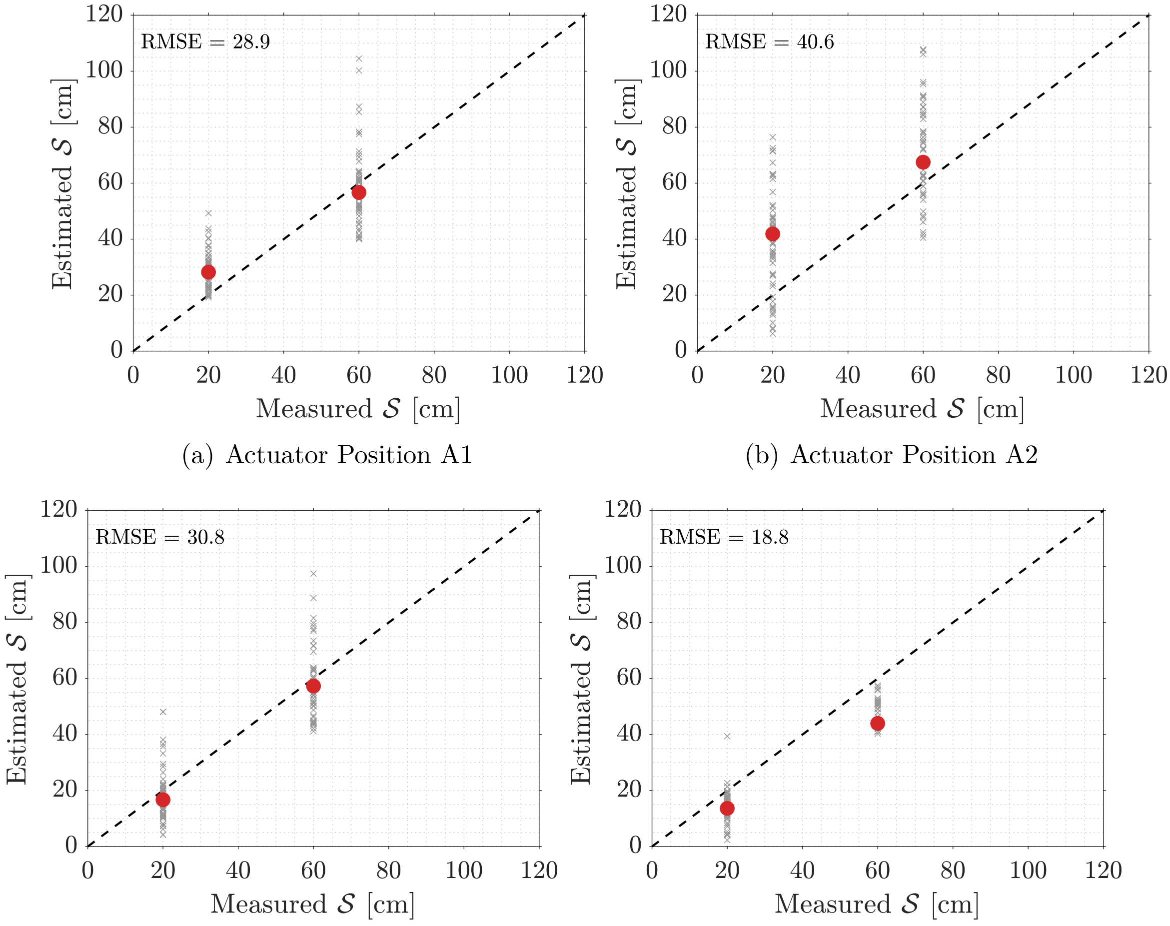

(a) Actuator Position A1

(b) Actuator Position A2

(c) Actuator Position A3

(d) Actuator Position A4

Source: Prepared by the author.

Table 6: Mean of estimated damage size and mean absolute error of prediction for test conditions (D20 and D60).

Actuator Position	A1		A2		A3		A4	
Condition	D20	D60	D20	D60	D20	D60	D20	D60
Mean of estimated damage size [cm]	28.75	58.70	39.69	70.47	17.77	60.18	14.32	46.02
Mean absolute error [cm]	8.78	9.77	22.05	14.71	6.78	11.46	6.38	13.97

Source: Prepared by the author.

presented in Figure 23 considering the four actuator positions. The estimated percentage of damage size using the damage indices from test conditions converged on the diagonal line. The RMSE value of the GPR model prediction considering the four actuator positions reveled a minimum value at actuator position A4, 18.8 mm, and maximum value at position A2, 40.6 mm. This indicates a better damage quantification overall performance of the GPR trained using data when the structure is excited at position A4.

The assessment of the prediction performance in each test condition is presented in Table 6, where it is showed the mean of the estimated and the mean absolute error of the damage size prediction. As can be observed, the mean of the estimated damage sizes remained close to the actual sizes, respectively, 20 cm and 60 cm. The mean absolute error of each condition showed a lower error for condition D20 at actuator position A4 and condition D60 at actuator position A1.

4.4 Conclusions

This chapter presented the modified damage quantification methodology based on the application of the GPR model. The methodology is applied in the SSP 34m wind turbine blade dataset. The damage feature extraction is performed based on the methodology proposed by Garcia and Tcherniak (2019). A global damage index is proposed to merge the information contained in all local paths considering each actuator position. The GPR model is used to capture the trend and uncertainties between the damage index and damage size. Although a reduced number of damaged conditions were available on the dataset, only six, from which four were utilized in the training step of the methodology, the GPR model demonstrated to be able to capture the trend and uncertainties between the global damage index adequately proposed and the damage size. The results of damage size estimation using the GPR model in the test step revealed better performance for the actuator at positions A1 and A4.

5 FINAL REMARKS

5.1 Conclusions

This work addressed the damage quantification in laminated composites with a novel methodology rooted in the stochastic interpolation of global damage indices based on the GPR model's application. The methodology is limited to the problem of damage quantification in the hotspot region, i.e., the damage localization is known a priori based on previous data. In the central methodology proposed for the problem of delamination area quantification in composite plates, AR model identification of Lamb wave signals is used for damage feature extraction. The damage indices are computed based on the MSD set for a reference condition; then, a trend curve is established using the GPR model to associate the damage index with the estimated delamination area with a confidence interval.

The first example performed in a carbon-epoxy laminate assuming temperature effects proved that the GPR could adequately capture the damage indices' regression trend. Some intermediary values of simulated damage not used in the training step were employed for validation. It was observed that the uncertainty interval could accommodate the estimate of damage progression. The second example was performed with a set of CFRP coupons with actual delamination caused by a tension-tension fatigue test, confirmed by X-ray tests. In this scenario, data measured in three coupons were used to train the stochastic regression, and another one was used to validate the estimate of the delamination area. The trained model captured the regression trend adequately, even in a more complex scenario with real damage.

The results found in both experiments confirmed that the learned model is useful to estimate the delamination area by stochastic interpolation in identical or nominally identical structures through damage indices. In all tests, the delamination area was identified suitably correlated with the proposed damage indices, despite the various sources of non-controlled uncertainties associated with the operational and environmental conditions. For this reason, this approach seems to be very appealing in industrial cases from the real-world for hotspot monitoring of the delamination area.

Moreover, the modified methodology for damage quantification based on the GPR model using vibration-based damage indices demonstrated to be useful in estimating the damage size in the SSP 34m wind turbine blade dataset. This demonstrates the versatility of the proposed methodology based on the GPR model's application, which can be extended for different damage features extraction techniques and damage types.

However, the limitations of the methodology proposed should be emphasized. The methodology is based on the supervised learning of the GPR model, which requires data from progressive damaged conditions of the structure that can be extremely expensive to obtain. Although the GPR model could capture the trend and uncertainties associated with the damage index and estimate the damage size adequately, the experiments were performed under controllable environmental/operational conditions. Then, it is expected an adequate performance under similar conditions. Moreover, the damage quantification is focused on the scenario of hotspot monitoring, i.e., the damage localization is known a priori based on previous data. Although this scenario simplifies the SHM methodology by eliminating the damage localization level, it is still of great technological importance.

5.2 Suggestions for Future works

Some suggestions of topics for future works are provided based on the results presented in this work:

- The methodology proposed in this work is based on a supervised approach to train the GPR model, which is performed using experimental data. However, in some cases, to obtain experimental data of progressive damaged conditions is too complex and expensive to reproduce. A suggestion to overcome this drawback is to study the application of data from the finite element model to train the GPR model.

- In the practical application proposed using nominally identical structures; it was observed a large variability of the damage indices computed, which affects the training of the GPR model. To address this problem, it should be interesting to apply algorithms for transfer learning to reduce the variability observed of the damage index computed in the different structures.

- Lamb wave propagation is greatly affected by operational/environmental variations, reflected in the damage index computed that compromises the methodology's performance. In this context, the application of a damage index using a relative free-baseline strategy proposed by Park *et al.* (2010) could be an interesting strategy to reduce the effects of operational/environmental conditions and to increase the robustness of the methodology.

- The application of the Polynomial-Chaos-Kriging model to improve the accuracy of the stochastic interpolation in the damage quantification methodology.

REFERENCES

AMER, A.; KOPSAFTOPOULOS, F. Probabilistic damage quantification via the integration of non-parametric time-series and gaussian process regression models. In: International Workshop on Structural Health Monitoring (IWSHM), 12., 2019, Stanford. **Proceedings [...]**, Stanford: DEStech Publications, p. 100, 2019. Available from: https://doi.org/10.12783/shm2019/32379. Access on: 15 Feb. 2020.

CANO, W. F. R.; SILVA, S. da. Fuzzy clustering and AR models for damage detection in CFRP coupons considering loading effect. **Journal of the Brazilian Society of Mechanical Sciences and Engineering**, Rio de Janeiro, v. 42, n. 5, 2020. Available from: https://doi.org/10.1007%2Fs40430-020-02304-7. Access on: 1 Ago. 2020.

CHEN, J.; YUAN, S.; WANG, H. On-line updating gaussian process measurement model for crack prognosis using the particle filter. **Mechanical Systems and Signal Processing**, London, v. 140, p. 106646, 2020. ISSN 0888-3270. Available from: http://www.sciencedirect.com/science/article/pii/S0888327020300327. Access on: 1 Jul. 2020.

CORBETTA, M.; SAXENA, A.; GIGLIO, M.; GOEBEL, K. An investigation of strain energy release rate models for real-time prognosis of fiber-reinforced laminates. **Composite Structures**, London, v. 165, p. 99 – 114, 2017. ISSN 0263-8223. Available from: http://www.sciencedirect.com/science/article/pii/S0263822316321146. Access on: 14 Feb. 2019.

CORBETTA, M.; SBARUFATTI, C.; GIGLIO, M.; SAXENA, A.; GOEBEL, K. A bayesian framework for fatigue life prediction of composite laminates under co-existing matrix cracks and delamination. **Composite Structures**, London, v. 187, p. 58 – 70, 2018. ISSN 0263-8223. Available from: http://www.sciencedirect.com/science/article/pii/S0263822317324030. Access on: 25 Feb. 2019.

CRESPO, B. H. Damage sensing in blades. In: OSTACHOWICZ, W.; MCGUGAN, M.; SCHRÖDER-HINRICHS, J.-U.; LUCZAK, M. (Ed.). **MARE-WINT: New Materials and Reliability in Offshore Wind Turbine Technology**. Cham: Springer International Publishing, 2016. p. 25–52. ISBN 978-3-319-39094-9.

FARRAR, C. R.; WORDEN, K. **Structural health monitoring: a machine learning perspective**. Hoboken, New Jersey: John Wiley & Sons, Ltd, 2012. 654 p.

FARRAR, C. R.; WORDEN, K.; TODD, M. D.; GYUHAE, P.; NICHOLS, J.; ADAMS, D. E.; BEMENT, M. T.; FARINHOLT, K. **Nonlinear system identification for damage detection**. Los Alamos, 2007. Available from: https://www.osti.gov/servlets/purl/922532/. Access on: 17 Oct. 2018.

FIGUEIREDO, E.; FIGUEIRAS, J.; GYUHAE, P.; FARRAR, C.; WORDEN, K. Influence of the autoregressive model order on damage detection. **Computer-Aided Civil and Infrastructure Engineering**, Hoboken, v. 26, n. 3, p. 225–238, 2010. Available from: https://onlinelibrary.wiley.com/doi/abs/10.1111/j.1467-8667.2010.00685.x. Access on: 25 Feb. 2019.

FIGUEIREDO, E.; GYUHAE, P.; FARINHOLT, K. M.; FARRAR, C. R.; LEE, J.-R. Use of Time-Series Predictive Models for Piezoelectric Active-Sensing in Structural Health Monitoring Applications. **Journal of Vibration and Acoustics**, New York, v. 134, n. 4, 06 2012. ISSN 1048-9002. Available from: https://doi.org/10.1115/1.4006410. Access on: 27 Mar. 2019.

FIGUEIREDO, E.; PARK, G.; FIGUEIRAS, J.; FARRAR, C.; WORDEN, K. **Structural health monitoring algorithm comparisons using standard data sets**. Los Alamos, 2009. Available from: https://permalink.lanl.gov/object/tr?what=info:lanl-repo/lareport/LA-14393. Access on: 15 Fev. 2019.

FIGUREIDO, E. **Damage Identification in Civil Engineering Infrastructure under Operational and Environmental Conditions**. 2010. 226 p. Thesis (Ph. D.) — Universidade do Porto - Faculdade de Engenharia, Porto, 2010. Available from: http://hdl.handle.net/10216/58566.

FUENTES, R.; CROSS, E.; HALFPENNY, A.; BARTHORPE, R.; WORDEN, K. Autoregressive gaussian processes for structural damage detection. In: International Conference on Noise and Vibration Engineering, 26.,2014. **Proceedings [...]**, Leuven: KU Leuven - Department of Mechanical Engineering, p. 469–483, 2014. ISBN 9789073802919. Available from: http://past.isma-isaac.be/downloads/isma2014/papers/isma2014_0711.pdf. Access on: 15 Fev. 2020.

GARCIA, D.; TCHERNIAK, D. An experimental study on the data-driven structural health monitoring of large wind turbine blades using a single accelerometer and actuator. **Mechanical Systems and Signal Processing**, London, v. 127, p. 102 – 119, 2019. ISSN 0888-3270. Available from: http://www.sciencedirect.com/science/article/pii/S0888327019301530. Access on: 1 Jun. 2020.

GHRIB, M.; BERTHE, L.; MECHBAL, N.; RÉBILLAT, M.; GUSKOV, M.; ECAULT, R.; BEDREDDINE, N. Generation of controlled delaminations in composites using symmetrical laser shock configuration. **Composite Structures**, London, v. 171, p. 286 – 297, 2017. ISSN 0263-8223. Available from: https://doi.org/10.1016/j.compstruct.2017.03.039. Access on: 1 Feb. 2019.

GHRIB, M.; RÉBILLAT, M.; ROCHES, G. V. des; MECHBAL, N. Automatic damage type classification and severity quantification using signal based and nonlinear model based damage sensitive features. **Journal of Process Control**, London, 2018. ISSN 0959-1524. Available from: http://www.sciencedirect.com/science/article/pii/S0959152418301975. Access on: 25 Feb. 2020.

IHN, J.-B.; CHANG, F.-K. Detection and monitoring of hidden fatigue crack growth using a built-in piezoelectric sensor/actuator network: I. diagnostics. **Smart Materials and Structures**, Bristol, v. 13, n. 3, p. 609–620, may 2004. Access on: 17 Oct. 2018.

KITAGAWA, G. **Introduction to Time Series Modeling**. Boca Raton, Florida: CRC Press, 2010. ISBN 9781584889229.

LARROSA, C.; LONKAR, K.; CHANG, F.-K. In situ damage classification for composite laminates using gaussian discriminant analysis. **Structural Health Monitoring**, London, v. 13, n. 2, p. 190–204, 2014. Available from: `https://doi.org/10.1177/1475921713517288`. Access on: 17 Oct. 2018.

LATANIOTIS, C.; MARELLI, S.; SUDRET, B. **UQLAB User Manual – Kriging (Gaussian process modelling)**. Zurich, 2015. 53 p. Report UQLab-V0.9-105. Available from: `https://www.doi.org/10.13140/RG.2.1.4827.3120`. Access on: 21 Jul. 2019.

LEE, J.-S.; PARK, G.; KIM, C.-G.; FARRAR, C. R. Use of relative baseline features of guided waves for in situ structural health monitoring. **Journal of Intelligent Material Systems and Structures**, London, v. 22, n. 2, p. 175–189, 2011. Available from: `https://doi.org/10.1177/1045389X10395643`. Access on: 25 Feb. 2019.

LJUNG, L. **System Identification: Theory for the User**. 2. ed. London: Pearson Education, 1998. ISBN 9780132440530.

LYNCH, J. P. Design of a wireless active sensing unit for localized structural health monitoring. **Structural Control and Health Monitoring**, Oxford, v. 12, p. 405–423, 2005. Available from: `https://onlinelibrary.wiley.com/doi/abs/10.1002/stc.77`. Access on: 25 Feb. 2019.

MATTOS, C. L. C.; DAMIANOU, A.; BARRETO, G. A.; LAWRENCE, N. D. Latent autoregressive gaussian processes models for robust system identification. **IFAC-PapersOnLine**, Vienna, v. 49, n. 7, p. 1121 – 1126, 2016. ISSN 2405-8963. Available from: `http://www.sciencedirect.com/science/article/pii/S2405896316305602`. Access on: 17 Jul. 2019.

MITRA, M.; GOPALAKRISHNAN, S. Guided wave based structural health monitoring: A review. **Smart Materials and Structures**, Bristol, v. 25, n. 5, p. 053001, 2016. Available from: `https://doi.org/10.1088%2F0964-1726%2F25%2F5%2F053001`. Access on: 17 Oct. 2018.

MONTESANO, J.; CHU, H.; SINGH, C. V. Development of a physics-based multi-scale progressive damage model for assessing the durability of wind turbine blades. **Composite Structures**, London, v. 141, p. 50 – 62, 2016. ISSN 0263-8223. Available from: `http://www.sciencedirect.com/science/article/pii/S0263822316000246`. Access on: 15 Apr. 2019.

NARDI, D.; LAMPANI, L.; PASQUALI, M.; GAUDENZI, P. Detection of low-velocity impact-induced delaminations in composite laminates using auto-regressive models. **Composite Structures**, London, v. 151, p. 108 – 113, 2016. ISSN 0263-8223. Available from: `https://doi.org/10.1016/j.compstruct.2016.02.005`. Access on: 15 Apr. 2019.

NIELSEN, M.; ROCZEK-SIERADZAN, A.; JENSEN, F.; NIELSEN, P.; BERRING, P.; SIERADZAN, T.; ROUDNITSKI, V.; BITSCHE, R.; KNUDSEN, H.; RASMUSSEN, A.; RASMUSSEN, J.; ULDAHL, U.; ANDRLOVÁ, Z.; BRANNER, K.; BAK, C.; KALLESØE, B.; MCGUGAN, M.; LAGERBON, M.; WEDEL-HEINEN, J.;

LINDBY, T.; RIBER, H.; JENSEN, C. **Full Scale Test SSP 34m blade, edgewise loading LTT. Extreme load and PoC_InvE Data report**. Roskilde, 2010. Danmarks Tekniske Universitet, Risø Nationallaboratoriet for Bæredygtig Energi. Available from: https://orbit.dtu.dk/en/publications/full-scale-test-ssp-34m-blade-edgewise-loading-ltt-extreme-load-a. Access on: 15 Jun. 2020.

PAIXÃO, J.; SILVA, S. Extrapolation of autoregressive models for structural health monitoring in composite structures. In: International Symposium on Solid Mechanics, 7., 2019, São Carlos. **Proceedings [...]**, São Carlos: [s.n.], 2019. Available from: https://doi.org/10.26678/ABCM.MECSOL2019.MSL19-0166. Access on: 15 Mai. 2019.

PAIXAO, J.; SILVA, S. D.; FIGUEIREDO, E. Damage quantification in composite structures using autoregressive models. In: WAHAB, M. A. (Ed.). **Proceedings of the 13th International Conference on Damage Assessment of Structures**. Singapore: Springer Singapore, 2020. p. 804–815. ISBN 978-981-13-8331-1. Available from: https://doi.org/10.1007/978-981-13-8331-1_63. Access on: 15 Apr. 2020.

PARK, G.; FIGUEIREDO, E.; FARINHOLT, K. M.; FARRAR, C. R. Time series predictive models of piezoelectric active-sensing for SHM applications. **Health Monitoring of Structural and Biological Systems 2010**, Bellingham: SPIE, v. 7650, p. 32 – 43, 2010. Available from: https://doi.org/10.1117/12.847690. Access on: 22 Mai. 2019.

RAMADAS, C.; BALASUBRAMANIAM, K.; JOSHI, M.; KRISHNAMURTHY, C. V. Interaction of the primary anti-symmetric lamb mode with symmetric delaminations: numerical and experimental studies. **Smart Materials and Structures**, Bristol, v. 18, n. 8, p. 085011, 2009. Available from: https://doi.org/10.1088%2F0964-1726%2F18%2F8%2F085011. Access on: 17 Oct. 2018.

RASMUSSEN, C. E. Gaussian processes in machine learning. In: BOUSQUET, O.; LUXBURG, U. von; RÄTSCH, G. (Ed.). **Advanced Lectures on Machine Learning**. Berlin: Springer Berlin Heidelberg, 2004. p. 63–71. ISBN 978-3-540-28650-9. Available from: https://doi.org/10.1007/978-3-540-28650-9_4. Access on: 23 Mai. 2019.

RYTTER, A. **Vibrational Based Inspection of Civil Engineering Structures**. 1993. 193 p. Thesis (Ph. D.) — University of Aalborg, Denmark, 1993.

SALAMONE, S.; BARTOLI, I.; SCALEA, F. L. D.; COCCIA, S. Guided-wave health monitoring of aircraft composite panels under changing temperature. **Journal of Intelligent Material Systems and Structures**, London, v. 20, n. 9, p. 1079–1090, 2009. Available from: https://doi.org/10.1177/1045389X08101634. Access on: 25 Feb. 2019.

SAXENA, A.; GOEBEL, K.; LARROSA, C.; JANAPATI, V.; ROY, S.; CHANG, F. Accelerated aging experiments for prognostics of damage growth in composite materials. **Proceedings of the 8th International Workshop on Structural Health Monitoring**, [S.l.]: DEStech Publications Inc., v. 2, p. 1283–91, 2011.

SAXENA, A.; GOEBEL, K.; LARROSA, C. C.; CHANG, F.-K. **CFRP Composites Data Set**. Moffett Field, 2011. NASA Ames Prognostics Data Repository, NASA Ames

Research Center. Available from: http://ti.arc.nasa.gov/tech/dash/groups/pcoe/prognostic-data-repository/. Access on: 10 Feb. 2019.

SCALEA, F. Lanza di; SALAMONE, S. Temperature effects in ultrasonic lamb wave structural health monitoring systems. **The Journal of the Acoustical Society of America**, New York, v. 124, n. 1, p. 161–174, 2008. Available from: https://doi.org/10.1121/1.2932071. Access on: 12 Mai. 2019.

SI, L.; WANG, Q. Rapid multi-damage identification for health monitoring of laminated composites using piezoelectric wafer sensor arrays. **Sensors**, Basel, v. 16, n. 5, 2016. ISSN 1424-8220. Available from: https://www.mdpi.com/1424-8220/16/5/638. Access on: 21 Jun. 2019.

SILVA, M. **Machine learning algorithms for damage detection in structures under changing normal conditions**. 2017. 80 p. Thesis (Ph. D.) — Universidade Federal do Pará, Belém, 2017. Available from: http://repositorio.ufpa.br:8080/jspui/handle/2011/8993. Access on: 18 Ago. 2019.

SILVA, S. D. Data-driven model identification of guided wave propagation in composite structures. **Journal of the Brazilian Society of Mechanical Sciences and Engineering**, Rio de Janeiro, v. 40, n. 11, p. 543, Oct 2018. ISSN 1806-3691. Available from: https://doi.org/10.1007/s40430-018-1462-4. Access on: 22 Sep. 2018.

SILVA, S. D.; JUNIOR, V. L.; JUNIOR, M. D. Structural health monitoring in smart structures through time series analysis. **Structural Health Monitoring**, London, v. 7, n. 3, p. 231–244, 2008. Available from: https://doi.org/10.1177/1475921708090561. Access on: 6 Sep. 2018.

SILVA, S. D.; PAIXÃO, J. A. S.; RÉBILLAT, M.; MECHBAL, N. Data-driven autoregressive model identification for structural health monitoring in anisotropic composite plates. In: Thematic Conference on Smart Structures and Materials - SMART, 9., 2019, Paris. **Proceedings [...]**, Paris: Artes Gráficas Torres S.L, p. 1213–1223, 2019. Available from: http://congress.cimne.com/smart2019/frontal/doc/EbookSMART2019.pdf. Access on: 5 Ago. 2019.

SOHN, H.; FARRAR, C. R. Damage diagnosis using time series analysis of vibration signals. **Smart Materials and Structures**, Bristol, v. 10, n. 3, p. 446–451, jun 2001. Available from: https://doi.org/10.1088%2F0964-1726%2F10%2F3%2F304. Access on: 7 Feb. 2019.

SU, Z.; YE, L. **Identification of damage using Lamb waves: from fundamentals to applications**. London: Springer Science & Business Media, 2009. ISBN 978-1-84882-783-7. Available from: https://doi.org/10.1007/978-1-84882-784-4.

TIAN, Z.; YU, L.; LECKEY, C. Delamination detection and quantification on laminated composite structures with lamb waves and wavenumber analysis. **Journal of Intelligent Material Systems and Structures**, London, v. 26, n. 13, p. 1723–1738, 2015. Available from: https://doi.org/10.1177/1045389X14557506. Access on: 30 Jul. 2019.

TOYAMA, N.; NODA, J.; OKABE, T. Quantitative damage detection in cross-ply laminates using lamb wave method. **Composites Science and Technology**, Oxford, v. 63, n. 10, p. 1473 – 1479, 2003. ISSN 0266-3538. Available from: http://www.sciencedirect.com/science/article/pii/S0266353803001635. Access on: 15 Jun. 2019.

ULRIKSEN, M. D.; TCHERNIAK, D.; KIRKEGAARD, P. H.; DAMKILDE, L. Operational modal analysis and wavelet transformation for damage identification in wind turbine blades. **Structural Health Monitoring**, London, v. 15, n. 4, p. 381–388, 2016. Available from: https://doi.org/10.1177/1475921715586623. Access on: 6 Sep. 2019.

VALENCIA, L. D. A.; CHATZI, E. N.; TCHERNIAK, D. Gaussian process models for mitigation of operational variability in the structural health monitoring of wind turbines. **Mechanical Systems and Signal Processing**, London, v. 142, p. 106686, 2020. ISSN 0888-3270. Available from: http://www.sciencedirect.com/science/article/pii/S0888327020300728. Access on: 1 Jun. 2020.

WORDEN, K.; MANSON, G.; FIELLER, N. Damage detection using outlier analysis. **Journal of Sound and Vibration**, London, v. 229, n. 3, p. 647 – 667, 2000. ISSN 0022-460X. Available from: http://www.sciencedirect.com/science/article/pii/S0022460X99925142. Access on: 5 Jun. 2019.

YADAV, S. K.; CUNG, H.; KOPSAFTOPOULOS, F.; CHANG, F.-K. Damage quantification of active sensing acousto-ultrasound-based shm based on a multi-path unit-cell approach. In: International Workshop on Structural Health Monitoring (IWSHM), 11., 2017, Stanford. **Proceedings [...]**, Stanford: DEStech Publications, 2017. Available from: https://doi.org/10.12783/shm2017/14218.

YADAV, S. K.; MISHRA, S.; KOPSAFTOPOULOS, F.; CHANG, F.-K. Reliability of crack quantification via acousto-ultrasound active-sensing structural health monitoring using surface-mounted pzt actuators/sensors. **Structural Health Monitoring**, London, v. 0, n. 0, p. 1475921720921536, 2020. Available from: https://doi.org/10.1177/1475921720921536. Access on: 6 Jul. 2020.

YUAN, F.-G. **Structural Health Monitoring (SHM) in Aerospace Structures**. Sawston: Woodhead Publishing, 2016. ISBN 978-0-08-100148-6. Available from: https://doi.org/10.1016/C2014-0-00994-X.

YUAN, S.; WANG, H.; CHEN, J. A pzt based on-line updated guided wave - gaussian process method for crack evaluation. **IEEE Sensors Journal**, Piscataway, v. 20, n. 15, p. 8204–8212, 2019. ISSN 2379-9153. Available from: https://doi.org/10.1109/JSEN.2019.2960408. Access on: 1 Jun. 2020.

ZHENG, W. X. Study of a least-squares-based algorithm for autoregressive signals subject to white noise. **Mathematical Problems in Engineering**, London, v. 2003, p. 93–101, 2003. Available from: https://doi.org/10.1155/S1024123X03210012. Access on: 15 Apr. 2019.

A DETAILS ON THE IDENTIFICATION OF AUTOREGRESSIVE MODEL

The choice of an appropriate model order is most crucial for the successful identification of an AR model. The choice is not unique and must be based on an understanding of the criterion selected, which will be addressed in this chapter. Various techniques have been proposed in the literature to address this problem, depending on the type of application.

Once the model order has been selected, the AR model identification procedure provides the best model available. However, the crucial question is whether the model is good enough. To address this question is necessary to evaluate the model, which is known as model validation, that will be addressed in the second section of this chapter.

A.1 AR model order estimation

The first step for the AR model identification is to define an adequate model order. The appropriate model order is initially unknown, and their choice has to be addressed carefully. A lower-order model will not be able to fit the signal and capture the signal's underlying dynamics. On the other hand, a higher-order can fit the signal, but may not generalize well to slight variation in the signals (FIGUEIREDO *et al.*, 2012). The most used techniques in the literature to address this problem are the Bayesian Information Criterion (BIC) and the Akaike Information Criterion (AIC).

The Bayesian Information Criterion (BIC) is a statistical measure for the comparative evaluation among time-series predictive models, such as AR models. This criterion measures the relative goodness of fit of a particular AR model(FIGUEIREDO *et al.*, 2009). The BIC of an AR model with order p is defined as:

$$BIC(p) = \ln\left|\sigma_{\varepsilon}^{2}\right| + k\ln T \tag{30}$$

σ_{ε}^{2} is the variance of the residuals, k is the number of coefficients estimated, and T is the number of samples. The BIC's first term measured the difference between the log-likelihood of the fitted model and the log-likelihood of the model under consideration.

The second term is a penalty term, which penalizes the order, i.e., the coefficients. The best model order is that one which minimizes the BIC.

The BIC computed for the signals from the application case I are presented in Fig. 24. As can be observed, the BIC function is not minimized in the plotted window, compromising the choice of the optimal model order. This common issue requires an interpretation of the model order selection (FIGUEIREDO *et al.*, 2010). It is impossible to establish a unique solution, as the BIC functions suggest that the model order could be in the range of 20 - 50. Figueiredo *et al.* (2012) proposed an algorithm to address this problem and automate the model order selection. This algorithm will be presented and discussed below.

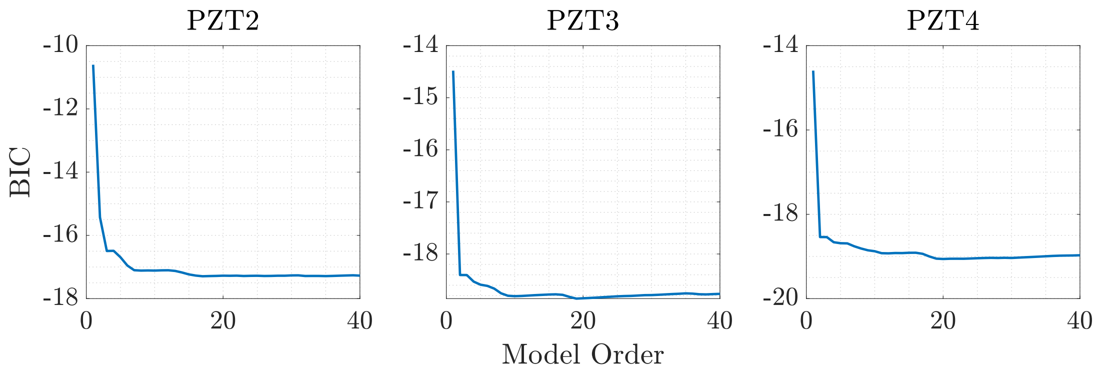

Figure 24: BIC computed from signals under baseline condition for application case I.

The algorithm for model order selection presented here was proposed by Figueiredo *et al.* (2009), and it is implemented in the software *SHMTools*. Fig. 25 illustrates schematically how the algorithm works. Firstly, it is necessary to define a maximum model order to be evaluated and the tolerance of convergence in the minimum searching algorithm. Then, an AR model for each order from one until the maximum defined is identified, and the respective BIC value is computed and stored in a vector. After that, the absolute difference between the first and the last value on the BIC vector is computed. Finally, the searching algorithm looks for the first element on the BIC vector less than BIC(end)+D*TOL. Then the index of the found element is the selected optimal order p for the AR model.

Tables 7 and 8 show the optimized order computed for all paths in the application case I and II respectively based on the algorithm presented previously. As can be observed, the optimal model order does not show a significant variation between the paths. For this reason, the AR model identification in SHM proposed was performed using just a single model order selected as the maximum order among those presented in the following path for each application case. Thus, it was selected the model orders of 18 and 16 for the application case I and II, respectively.

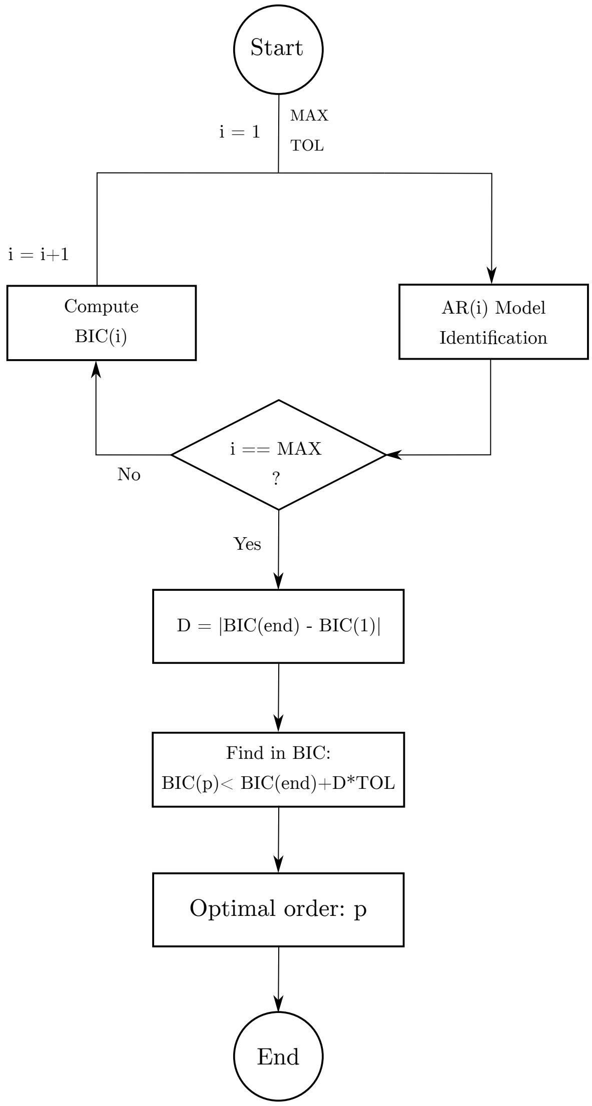

Figure 25: Algorithm of model order selection based on BIC.

A.2 Model validation

The AR model validation objective is to verify if the model is good enough in reproducing the identified signal. The method to perform this verification is to confront the estimated model with as much information the actual system has in practical (LJUNG, 1998). It is important to note that in the model validation, the signal used as a reference in the comparison should be different from that used in the model identification, and it is named as validation signal. In this work, a two-step model validation is proposed, based on the techniques presented in Ljung (1998): (1) goodness of fit evaluation; and (2) residual analysis.

Input PZT	1		
Output PZT	2	3	4
Optimal Order	16	8	**18**

Table 7: Optimized model order computed based on BIC for each path in the application case I. The value in bold highlighted represents the model order selected for AR model identification in this application case.

Input PZT	1						2						3					
Output PZT	7	8	9	10	11	12	7	8	9	10	11	12	7	8	9	10	11	12
Optimal Order	15	15	15	15	15	15	15	**16**	15	14	15	15	15	14	14	14	15	15

Input PZT	4						5						6					
Output PZT	7	8	9	10	11	12	7	8	9	10	11	12	7	8	9	10	11	12
Optimal Order	15	14	14	14	14	16	15	15	14	14	16	16	15	15	14	14	16	14

Table 8: Optimized model order computed based on BIC for each path in the application case I. The value in **bold** highlighted represents the model order selected for AR model identification in this application case.

The evaluation of the goodness of fit consists of comparing the estimated and the validation signal through a statistic measure. A standard metric applied which will be used in this work is the normalized mean square error (NMSE), which is defined as:

$$NMSE = 1 - \frac{\|y(k) - \hat{y}(k)\|^2}{\|y(k) - \bar{y}(k)\|^2} \tag{31}$$

, where $y(k)$ is the signal for validation, $\hat{y}(k)$, is the estimated signal, and $\bar{y}(k)$ is the mean of the validation signal. $NMSE$ can take on any value between 0 and 100, with a value closer to 100, indicating a better model fit.

The second step of the model validation consists of the residual analysis. This technique is commonly used in the field of time-series predictive models, such as AR models.

In the AR model identification, the part of the data that the model could not reproduce are the residuals (LJUNG, 1998):

$$\varepsilon = y(t) - \hat{y}(t) \tag{32}$$

where y is the data and $\hat{y}$ is the predicted value by the identified model at the instant t. The residuals carry information about the quality of the model.

As stated in Chapter 2, if an AR model is adequately identified, the residuals should be white noise, i.e., independent of each other. Based on this assumption, a simple test of this hypothesis consists of the whiteness test, which is performed by evaluating the autocorrelation function (ACF) of the residuals (LJUNG, 1998):

$$\hat{R}_k = \frac{1}{T\sigma^2} \sum_{t=1}^{T-k} [\varepsilon(t) - \bar{\varepsilon}][\varepsilon(t+k) - \bar{\varepsilon}] \tag{33}$$

where $\bar{\varepsilon}$ is the mean of residuals, T is the total number of samples, σ^2 is the variance of the residuals, t is the residual sample number and k the lag number of ACF. The ACF holds the $k = 0$ is one. If the ACF for $k = 0$ stays close to 0 along, it indicates that the residuals are independent of each other, i.e., it is a white noise process (LJUNG, 1998).

B LABVIEW APPLICATION

This appendix presents the application developed in *Labview* to control the instruments utilized in the experimental setup to generate and acquire the signals of Lamb wave propagation. Figure 26 presents the front panel of the application, where the user can set up the parameters related to the signal generation, acquisition, and data saving. Furthermore, the user can choose the number of acquired signal in each test by changing the number of repetitions and visualize the acquired signals on the two graphs. Fig. 27 shown the block diagram from the *Labview* application.

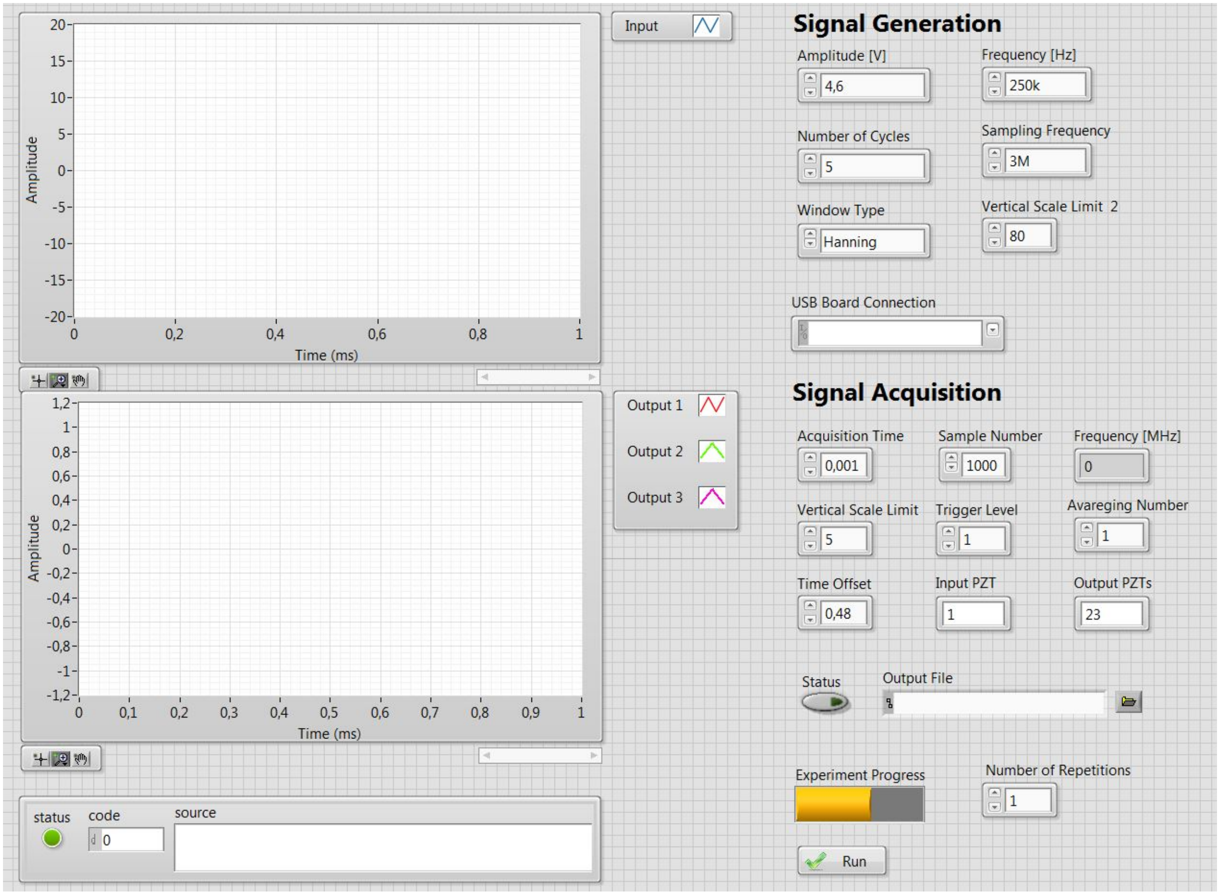

Figure 26: Front panel of Labview application

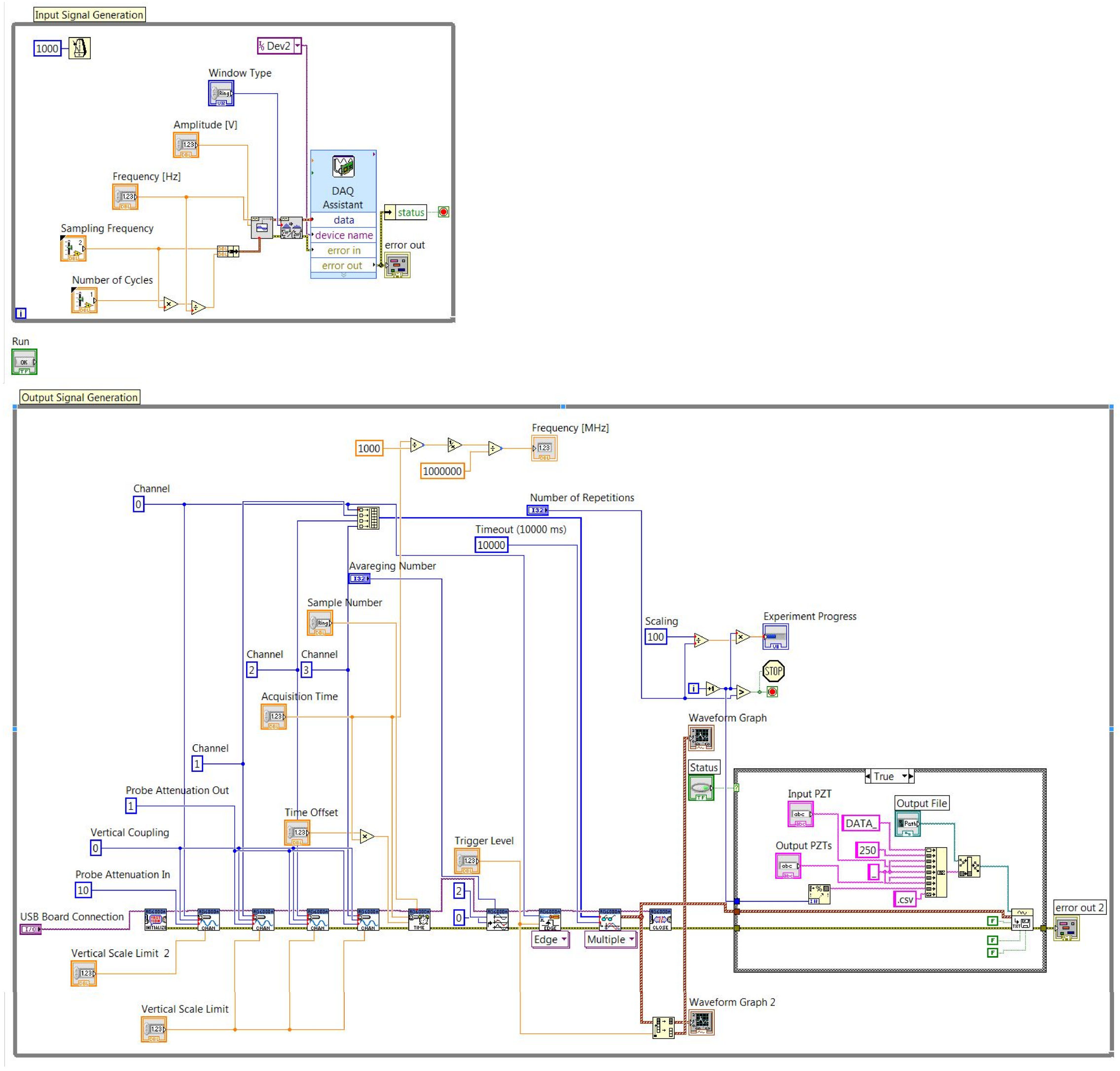

Figure 27: Block diagram of Labview application.

C PUBLICATIONS

In the development of this project it was published the following conference papers :

- Paixão J.A.S., Villani L.G.G., da Silva S. (2018) Damage Analysis in a Composite Plate Using Autoregressive models. Symposium on Intelligent Materials and Control - SIMC 2018. UNESP - FEIS, Ilha Solteira. Available on: <https://www.feis.unesp.br/#!/departamentos/engenharia-mecanica/grupos/simc/programacao/>

- Paixão J.A.S., da Silva S. (2019) Extrapolation of Autoregressive Models for Structural Health Monitoring in Composite Structures. In: Proceedings of the 7th International Symposium on Solid Mechanics. ABCM. Available on: <doi://10.26678/ABCM.MECSOL2019.MSL19-0166>

- Paixão J.A.S., da Silva S., Figueiredo E., Radu L., Park G. (2019) Probabilistic damage quantification in composite structures using Gaussian process regression. In: 2019 Fall Conference and 39th Regular General Meeting. Korean Society for Nondestructive Testing (KSNT) . Available on: <http://ksnt.or.kr/Conference/ConferenceView.asp?AC=0&CODE=CC20190901&CpPage=553#CONF>

- Da Silva S.,Paixão J.A.S., Rebillat M., Mechball N. (2019) Data-driven autoregressive model identification for structural health monitoring in anisotropic composite plates. In: IX ECCOMAS Thematic Conference on Smart Structures and Materials SMART 2019, 2019, Paris. SMART 2019. Barcelona, Spain: Artes Gráficas Torres S.L., 2019. p. 1213-1223.

- Paixão J.A.S., da Silva S., Figueiredo E. (2020) Damage Quantification in Composite Structures Using Autoregressive Models. In: Wahab M. (eds) Proceedings of the 13th International Conference on Damage Assessment of Structures. Lecture Notes in Mechanical Engineering. Springer, Singapore. Available on: <https://doi.org/10.1007/978-981-13-8331-1_63>

The following paper : 'Delamination area quantification in composite structures using Gaussian process regression and AR models'; which contains the results presented in the Chapters 2 and 3 of this work was submitted to the Journal of Vibration and Control. A new paper related with the results presented in Chapter 4 of this work is being prepared and it will be submitted soon for the Structural Health Monitoring Journal. Furthermore, two research internships abroad were performed during the period of this research project : the first one held in Lisbon (Portugal) for one month at Universidade Lusófona de Humanidades e Tecnologia supervised by Prof. Dr. Eloi Figueiredo; and the second, lasting three months in Gwangju (South Korea) supervised by Prof. Dr. Gyuhae Park supported by FAPESP (Grant 2019/11755-9).